J. Math. Biol. 41, 45–79 (2000)
Digital Object Identifier (DOI):
10.1007/s002850000044

Mathematical Biology

© Springer-Verlag 2000

J.J. Batzel · H.T. Tran

Stability of the human respiratory control system

I. Analysis of a two-dimensional delay state-space model

Received: 4 January 1999 / Revised version: 25 August 1999 /
Published online: 4 July 2000

Abstract. A number of mathematical models of the human respiratory control system have been developed since 1940 to study a wide range of features of this complex system. Among them, periodic breathing (including Cheyne-Stokes respiration and apneustic breathing) is a collection of regular but involuntary breathing patterns that have important medical implications. The hypothesis that periodic breathing is the result of delay in the feedback signals to the respiratory control system has been studied since the work of Grodins et al. in the early 1950's [12]. The purpose of this paper is to study the stability characteristics of a feedback control system of five differential equations with delays in both the state and control variables presented by Khoo et al. [17] in 1991 for modeling human respiration. The paper is divided in two parts. Part I studies a simplified mathematical model of two nonlinear state equations modeling arterial partial pressures of O_2 and CO_2 and a peripheral controller. Analysis was done on this model to illuminate the effect of delay on the stability. It shows that delay dependent stability is affected by the controller gain, compartmental volumes and the manner in which changes in the ventilation rate is produced (i.e., by deeper breathing or faster breathing). In addition, numerical simulations were performed to validate analytical results. Part II extends the model in Part I to include both peripheral and central controllers. This, however, necessitates the introduction of a third state equation modeling CO_2 levels in the brain. In addition to analytical studies on delay dependent stability, it shows that the decreased cardiac output (and hence increased delay) resulting from the congestive heart condition can induce instability at certain control gain levels. These analytical results were also confirmed by numerical simulations.

1. Introduction and modeling considerations

The human respiratory system acts to exchange carbon dioxide, CO_2, which is the unwanted gas byproduct of metabolism for oxygen, O_2, which is necessary for metabolism. The control mechanism which responds to the changing needs of the body to acquire oxygen, O_2 and to expel carbon dioxide, CO_2, acts to modulate the ventilation rate, which will be denoted by $\dot{V}_I$, in a manner designed to maintain normal levels of these gases. In the absence of voluntary control of breathing or neurological induced changes in breathing, the respiratory control system varies

J.J. Batzel, H.T. Tran: Center for Research in Scientific Computation, Department of Mathematics, Box 8205, North Carolina State University, Raleigh, NC 27695-8205, USA.
e-mail: `jjbatzel@unity.ncsu.edu`; `tran@control.math.ncsu.edu`

Key words: Respiratory control models – Time delay – Delay-dependent stability – Instability – Numerical simulations

the ventilation rate in response to the levels of CO_2 and O_2. We refer to this system as the chemical control system and will consider its dynamics. Furthermore, chemical control is the only control regulating respiration during sleep, a state in which involuntary cessation of breathing (referred to as apnea) can occur.

There are two sites where CO_2 and O_2 levels are measured:

- The peripheral controller consists of the carotid receptors found in the angle of the bifurcation of the common carotid arteries, as well as chemoreceptors in the aortic arch. They respond to both O_2 and CO_2 via the partial pressures $P_{a_{CO_2}}$ and $P_{a_{O_2}}$ [20].
- The central controller responds exclusively to the partial pressure of carbon dioxide in the brain, $P_{B_{CO_2}}$ [20]. $P_{B_{CO_2}}$ stimulates certain brain cells in the medulla responsible for the control of ventilation [13]. Of course, $P_{B_{CO_2}}$ is related to $P_{a_{CO_2}}$ and the metabolic rate of CO_2 production in the brain. For the two dimensional model considered in Part I of this paper, the controlling quantity is $P_{a_{CO_2}}$.

These two sensor sites are located a physical distance from the lungs which is the site at which CO_2 and O_2 levels can be altered by means of varying the ventilation rate. Consequently, the feedback controller in the mathematical model will consist of two transport delays. In general, our analysis below does not depend on the actual form of the control equation so that different controls may be analyzed. We do, however, assume that the ventilation function, $\dot{V}_I$, satisfies:

(i) $\dot{V}_I \geq 0$;
(ii) $\dot{V}_I = \dot{V}_I(P_{a_{CO_2}}, P_{a_{O_2}})$ is an increasing function with respect to $P_{a_{CO_2}}$ and decreasing in $P_{a_{O_2}}$;
(iii) $\dot{V}_I$ has continuous partial derivatives except perhaps at $\dot{V}_I = 0$.

A number of minimal models have been devised to study stability of the respiratory system. Glass and Mackey [11,19] and Carley and Shannon [3] considered a one-dimensional state space model. Cleave et al. [4] studied a two-dimensional model. ElHefnawy et al. [9] considered a three-dimensional model for simulations which they reduced to a one-dimensional model for stability analysis. Each model mentioned above had strong points and weaknesses. When considering minimal models several features of the respiratory system in steady state need to be kept in mind.

(i) Peripheral ventilatory control response is 25% of the total response.
(ii) CO_2 sensitivity is around 2 liters/min/mmHg.
(iii) Total ventilation is 7 liters/min approximately.
(iv) $P_{a_{CO_2}}$ = 40 mmHg and $P_{a_{O_2}}$ = 95 to 100 mmHg approximately.
(v) $\dot{V}_I$ increases linearly with CO_2 and decreases exponentially with O_2.
(vi) The central control responds to the CO_2 in the brain which varies less than the arterial level of CO_2.

For minimal models it is difficult to satisfy all of these criteria simultaneously. For example, Glass and Mackey matched items (iii) and (iv) above but CO_2

sensitivity could vary by as much as 100% during oscillatory behavior. We note that Glass and Mackey, ElHefnawy et al. and Carley and Shannon considered only CO_2 control of ventilation. There are trade-offs in steady state values for Pa_{CO_2}, $\dot{V}_I$ and control gain. For example, if one considers only Pa_{CO_2} control then a control gain level sufficient to produce the correct steady state value of Pa_{CO_2} and $\dot{V}_I$ might make the control hypersensitive to changing Pa_{CO_2} levels. Cooke and Turi [5] considered a two-dimensional extension of the Glass and Mackey model which included a control responsive to both peripheral Pa_{CO_2} and Pa_{O_2}. They acknowledged that the system would be more unstable than the physiological system as the peripheral control responds rapidly to arterial gas levels. Our model, however, includes a more physiologically correct control equation and physiologically correct relation between arterial and venous levels of Pa_{CO_2} and Pa_{O_2} based on the model in [17].

The purpose of this paper is twofold. First, we want to understand how the delay inherent in the respiratory control system affects the stability of the system. Second, we analyze some of the structure of the physiological control to see how this structure works to maintain stability. We begin in Section 2 describing the Khoo et al. model [17] which consists of a nonlinear system of five delay differential equations with multiple delays modeling human respiration. This model was later extended by Batzel and Tran [1] to include variable cardiac output and to study infant sleep respiratory patterns including obstructive apnea and central apnea which may play a role in sudden infant death syndrome (SIDS). However, this model is too complicated for a stability study. Section 3.1 describes a simplified mathematical model consisting of two state variables modeling arterial partial pressures of CO_2 and O_2 and a peripheral controller. Analytical results and numerical studies on delay dependent stability analysis are given in Section 3.2 and Section 3.3, respectively. Section 3.4 describes a modified control model to include a central control component and its analytical and numerical results. Section 3.5 contains some parameter studies which are used in the discussion of stability results (see remarks following theorem 3.8). Additional discussions of our analysis are given in Section 4 and Section 5 contains our concluding remarks.

2. The five-dimensional state space model

In this section we briefly describe the five-dimensional model developed in [17]. This section forms the basis for the simplified model developed and analyzed in Section 3. The following symbol sets will be used throughout the paper.

Primary symbols

M = effective volume in compartment
MR = metabolic rate
P = partial pressure
Q = volume of blood
$\dot{Q}$ = volume of blood per unit time
V = volume of gas
$\dot{V}$ = volume of gas per unit time

Subscripts for gas or compartment phase

A = alveolar
AT = sea level air pressure
B = brain
C = carbon dioxide
D = dead space
E = expired
I = inspired
L = lung
O = oxygen
T = tissue

Subscripts for blood phase

a = mixed arterial
c = capillary
$\hat{c}$ = end-capillary
i = ideal
m = mixed
v = mixed venous

For example, Pa_{O_2} indicates arterial partial pressure of O_2 leaving the lungs and $\dot{V}_I$ represents the inspired ventilation rate. The equations for the model studied arise from straightforward development of mass balance equations utilizing Fick's law, Boyle's law and variations of Henry's law relating the concentration of a gas in the solution to the partial pressure of the gas interfacing with the solution. The model describes three compartments: the lung compartment, a general tissue compartment and a brain compartment. A block diagram describing the the relationships between the three compartments and transport delays is shown in Figure 1.

The equations describing the dynamics between the three compartments are given by:

$$\frac{dPa_{CO_2}(t)}{dt} = \frac{863\dot{Q}K_{CO_2}[Pv_{CO_2}(t-\tau_V) - Pa_{CO_2}(t)] + E_F\dot{V}_I[PI_{CO_2} - Pa_{CO_2}(t)]}{M_{L_{CO_2}}}, \tag{1}$$

$$\frac{dPa_{O_2}(t)}{dt} = \frac{863\dot{Q}[m_v Pv_{O_2}(t-\tau_V) - m_a Pa_{O_2}(t) + B_v - B_a]}{M_{L_{O_2}}} + \frac{E_F\dot{V}_I[PI_{O_2} - Pa_{O_2}(t)]}{M_{L_{O_2}}}, \tag{2}$$

$$\frac{dP_{B_{CO_2}}(t)}{dt} = \frac{MR_{B_{CO_2}}}{M_{B_{CO_2}}K_{B_{CO_2}}} + \frac{[\dot{Q}_B(Pa_{CO_2}(t-\tau_B) - P_{B_{CO_2}}(t))]}{M_{B_{CO_2}}}, \tag{3}$$

$$\frac{dPv_{CO_2}(t)}{dt} = \frac{MR_{T_{CO_2}}}{M_{T_{CO_2}}K_{CO_2}} + \frac{[\dot{Q}_T(Pa_{CO_2}(t-\tau_T) - Pv_{CO_2}(t))]}{M_{T_{CO_2}}}, \tag{4}$$

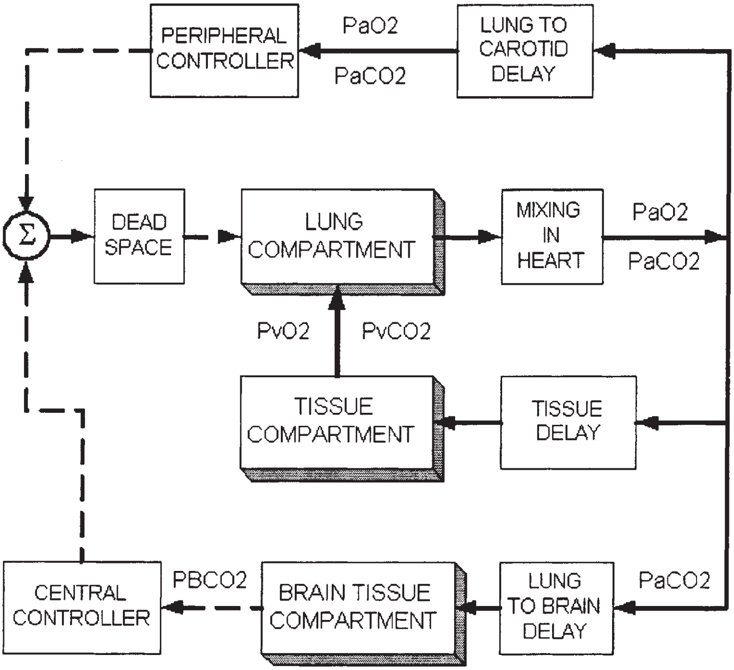

Fig. 1. Block diagram of the respiratory system model.

$$\frac{d\mathrm{Pv}_{\mathrm{O}_2}(t)}{dt} = \frac{\dot{\mathrm{Q}}_{\mathrm{T}}[\mathrm{m_a Pa}_{\mathrm{O}_2}(t-\tau_{\mathrm{T}}) - \mathrm{m_v Pv}_{\mathrm{O}_2}(t) + \mathrm{B_a} - \mathrm{B_v}] - \mathrm{MR}_{\mathrm{T}_{\mathrm{O}_2}}}{\mathrm{M}_{\mathrm{T}_{\mathrm{O}_2}}\mathrm{m_v}}. \quad (5)$$

Equations (1) and (2) describe the lung compartment partial pressures of CO_2 and O_2 respectively. Equations (4) and (5) describe the tissue compartment (including also brain tissue) partial pressures of CO_2 and O_2 respectively. Equation (3) describes the brain compartment CO_2 partial pressure. E_F, $P_{I_{O_2}}$, K_{CO_2}, m_a, m_v, B_a and B_v are constants. The constants K_{CO_2}, m_a, m_v, B_a and B_v occur in the so-called dissociation laws relating gas concentrations to partial pressures. $P_{I_{O_2}}$ represents inspired oxygen. We include an alveolar arterial gradient of 4 mmHg (unless otherwise indicated) by reducing $P_{I_{O_2}}$ by this amount [20]. The CO_2 dissociation law is assumed linear while the O_2 dissociation law is nonlinear but approximately piecewise linear. In the above model, it was assumed that the O_2 partial pressures stay within one band of the piecewise linear representation thus making it linear. Furthermore, the metabolic rates and compartment volumes are assumed constant. E_F reduces the effectiveness of ventilation and is used to model the effects of the ventilatory dead space. Ventilatory dead space refers to the fact that, on inspiration, one first brings into the alveoli air from the upper conducting airways (where no gas exchange occurs) left over from expiration. This air is fully equilibrated with the venous partial pressures of CO_2 and O_2 and hence does not contribute to the ventilation process. This dead space represents approximately 25–30% of the air moved during inspiration.

The ventilation rate $\dot{V}_I$ depends on the signals sent from the peripheral and central sensors and the peripheral and central control effects are additive [7]. Thus

$$\dot{V}_I = \dot{V}_{periph} + \dot{V}_{cent}, \tag{6}$$

where

$$\begin{aligned} \dot{V}_{cent} &= \text{ventilation due to the central control signal,} \\ \dot{V}_{periph} &= \text{ventilation due to the peripheral control signal.} \end{aligned}$$

Physiologically, we do not assign any meaning to a negative $\dot{V}_I$, $\dot{V}_{periph}$ or $\dot{V}_{cent}$. Let $\dot{V}_P$ be the function defining ventilation due to the peripheral control signal and $\dot{V}_C$ be the function defining ventilation due to the central control signal. Then, we set $\dot{V}_P$ and $\dot{V}_C$ equal to zero should these functions become negative. Using the following notation

$$[[x]] = \begin{cases} x & \text{for } x \geq 0 \\ 0 & \text{for } x < 0 \end{cases}.$$

the control equation actually takes the form

$$\dot{V}_I = [[\dot{V}_P]] + [[\dot{V}_C]]$$

where

$$\dot{V}_P = G_P \exp(-.05 Pa_{O_2}(t - \tau_a))(Pa_{CO_2}(t - \tau_a) - I_P)$$

and

$$\dot{V}_C = G_C(P_{B_{CO_2}}(t) - \frac{MR_{B_{CO_2}}}{K_{CO_2}\dot{Q}_B} - I_C).$$

Here, G_C and G_P are control gains and I_C and I_P are cutoff thresholds. However, to simplify our discussion, we will omit this notation while always maintaining that the peripheral and central ventilation rates will be greater than or equal to zero.

The control equation describing the rate of ventilation $\dot{V}_I$ is thus [17]

$$\begin{aligned} \dot{V}_I = {} & G_P \exp(-.05 Pa_{O_2}(t - \tau_a))(Pa_{CO_2}(t - \tau_a) - I_P) \\ & + G_C(P_{B_{CO_2}}(t) - \frac{MR_{B_{CO_2}}}{K_{CO_2}\dot{Q}_B} - I_C). \end{aligned} \tag{7}$$

The first term in (7) describes $\dot{V}_{periph}$ and the second term describes $\dot{V}_{cent}$.

3. A simplified two-dimensional state space model

3.1. Model equations

The mathematical model described in Section 2 has been used to study the mechanisms producing unstable patterns of breathing such as periodic breathing and apnea, and specifically to investigate numerically the hypothesis that such phenomena represent the manifestation of feedback-induced instabilities in the respiratory control system (see e.g. [15], [16], [17]). This model was later extended by Batzel and Tran [1] to include variable state dependent delay in the feedback control loop and to study the phenomena of periodic breathing and apnea as they occur during quiet sleep in infant sleep respiration at around 4 months of age. Although this model captures many physiological aspects of human respiration, it is very complex for a rigorous analytical study of the effect of delay on the stability. In this section, we simplified the model presented in Section 2 to include only two state variables: $\mathrm{Pa_{CO_2}}$ and $\mathrm{Pa_{O_2}}$. We make the following simplifying assumptions:

(i) $\mathrm{P_{V_{CO_2}}}$ = constant.
(ii) $\mathrm{P_{V_{O_2}}}$ = constant.
(iii) $\dot{\mathrm{Q}}$ = constant.
(iv) $\mathrm{O_2}$ values stay within one section of the dissociation piecewise function.
(v) The only delay is to the peripheral control.
(vi) Only the peripheral control is modeled.
(vii) The one delay to peripheral control is constant since $\dot{\mathrm{Q}}$ is constant.
(viii) There is no modeling of breath by breath changes (constant flow model).
(ix) Dead space ventilation is represented by the ventilation factor $\mathrm{E_F}$.

Assumptions (i) and (ii) above are fairly reasonable (even during oscillations) as can be seen in the full model simulations of adult Cheyne Stokes respiration shown in Figure 2 [1]. Specifically, the simulations were obtained by reducing the cardiac output by 50% from the normal case and thus doubling all transport delays in the full model (1)–(5).

This reduces the model to 3 state equations for $\mathrm{Pa_{CO_2}}$, $\mathrm{Pa_{O_2}}$ and $\mathrm{P_{B_{CO_2}}}$. We first consider only peripheral control (consequently, there is one transport delay). This eliminates the need for the equation for $\mathrm{P_{B_{CO_2}}}$. The reduced model will exhibit greater instability than would be the case for the full system (see section 3.4 for further discussion). We are left with the 2 equations describing $\mathrm{Pa_{CO_2}}$ and $\mathrm{Pa_{O_2}}$ and a control equation responsive to arterial $\mathrm{Pa_{CO_2}}$ and $\mathrm{Pa_{O_2}}$ with one transport delay to the peripheral controller. The system, with these assumptions, is a nonlinear, autonomous, two-dimensional system of ordinary differential equations with one constant delay. The state equations are:

$$\frac{d\mathrm{Pa_{CO_2}}(t)}{dt} = \frac{863\dot{\mathrm{Q}}\mathrm{K_{CO_2}}[\mathrm{P_{V_{CO_2}}} - \mathrm{Pa_{CO_2}}(t)]}{\mathrm{M_{L_{CO_2}}}} + \frac{\mathrm{E_F}\dot{\mathrm{V}}_\mathrm{I}[\mathrm{P_{I_{CO_2}}} - \mathrm{Pa_{CO_2}}(t)]}{\mathrm{M_{L_{CO_2}}}}, \tag{8}$$

$$\frac{d\mathrm{Pa_{O_2}}(t)}{dt} = \frac{863\dot{\mathrm{Q}}[\mathrm{m_v P_{V_{O_2}}} - \mathrm{m_a Pa_{O_2}}(t) + \mathrm{B_v} - \mathrm{B_a}]}{\mathrm{M_{L_{O_2}}}} + \frac{\mathrm{E_F}\dot{\mathrm{V}}_\mathrm{I}[\mathrm{P_{I_{O_2}}} - \mathrm{Pa_{O_2}}(t)]}{\mathrm{M_{L_{O_2}}}}. \tag{9}$$

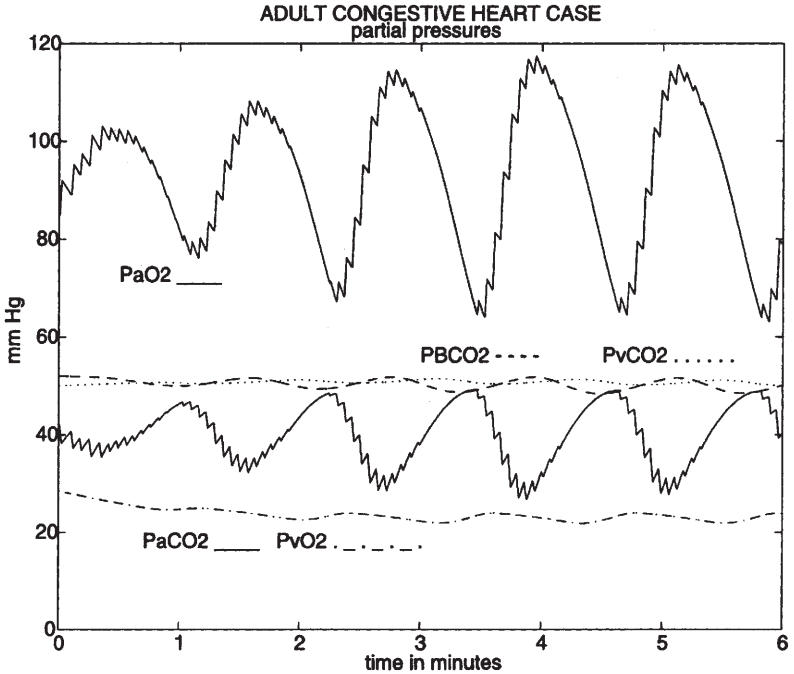

Fig. 2. Full model simulations of adult congestive heart case: periodic breathing.

Recalling the bracket notation from Section 2, the control equation is described as follows.

$$\dot{\mathrm{V}}_{\mathrm{I}} = [[\ \ \mathrm{G_P} \exp\left(-.05\mathrm{Pa_{O_2}}(t-\tau_{\mathrm{a}})\right)(\mathrm{Pa_{CO_2}}(t-\tau_{\mathrm{a}}) - \ \mathrm{I_P})\ \ ]].$$

Again, for simplicity of notation, we will drop the double brackets and simply write the control equation as

$$\dot{\mathrm{V}}_{\mathrm{I}} = \mathrm{G_P} \exp\left(-.05\mathrm{Pa_{O_2}}(t-\tau_{\mathrm{a}})\right)(\mathrm{Pa_{CO_2}}(t-\tau_{\mathrm{a}}) - \ \mathrm{I_P}),$$

Table 7 at the appendix section of this paper gives parameter values used in our simulation studies of this simplified model for human respiration.

3.2. Stability analysis of the two-dimensional state space model

Let $r \geq 0$ and $C([a,b], \mathbb{R}^{\mathrm{n}})$ be the Banach space of continuous functions mapping $[a,b]$ into $\mathbb{R}^{\mathrm{n}}$ with the sup norm $|\cdot|_\infty$. For simplicity of notation, we will denote $C([-r,0], \mathbb{R}^{\mathrm{n}})$ by C. For $\phi \in C$, define $|\phi| = \sup_{-r\leq\theta\leq 0} |\phi(\theta)|$. Let $B(0,b) = \{x|\ |x| \leq b\}$ for x in a normed space with norm $|\cdot|$. For $\sigma \in \mathbb{R}$, $\mathrm{A} \geq 0$, $x \in C([\sigma - r, \sigma + A],\ \mathbb{R}^{\mathrm{n}})$ and $t \in [\sigma, \sigma + A]$ define $x_t \in C$ by

$$x_t(\theta) = x(t+\theta).$$

We recall the following definitions of stability which will be needed in this section.

Suppose $f : \mathbb{R} \times C \to \mathbb{R}^{\mathrm{n}}$ with the sup norm $|\cdot|_\infty$ and consider the retarded functional differential equation

$$\dot{x}(t) = f(t, x_t). \tag{10}$$

For a given $\sigma \in \mathbb{R}$ and $\phi \in C$ we say $x(\sigma, \phi)$ is a solution of (10) with initial data $\phi \in C$ at σ if there is an $A > 0$ such that $x(\sigma, \phi)(t)$ satisfies (10) on $[\sigma - r, \sigma + A]$ and $x_\sigma(\sigma, \phi) = \phi$.

Definition 3.1. Suppose $f(t, 0) = 0$ for all $t \in \mathbb{R}$. The solution $x = 0$ of equation (10) is said to be *stable* if for any $\sigma \in \mathbb{R}$, $\epsilon > 0$, there is a $\delta = \delta(\epsilon, \sigma)$ such that $\phi \in B(0, \delta) \subset C$ implies $x_t(\sigma, \phi) \in B(0, \epsilon)$ for $t \geq \sigma$. The solution $x = 0$ of equation (10) is said to be *asymptotically stable* if it is stable and there is a $b_o = b_o(\sigma) > 0$ such that $\phi \in B(0, b_o)$ implies $x(\sigma, \phi)(t) \to 0$ as $t \to \infty$.

To study the stability properties of the nonlinear system (8) and (9), we will apply the following well-known theorems. A proof may be found in [10] (see Theorems (3.7.1) and (3.7.2)). Consider the system

$$\begin{aligned} \dot{x}_i(t) = {} & \sum_{j=1}^{n} \sum_{k=1}^{m} a_{ijk} x_j(t - \tau_k) \\ & + R_i(t, x_1(t), x_2(t - \tau_1), ...x_n(t - \tau_m)), \;\; i = 1, 2, \ldots, n \end{aligned} \tag{11}$$

and define the characteristic equation for this system as

$$|\sum_{k=1}^{m} A_k \exp\left(-\lambda \tau_k\right) - \lambda I| = 0,$$

where $A_k = (a_{ijk})$ are matrices and I is the identity matrix.

Theorem 3.1. *The null solution of the n dimensional system defined by (11) is asymptotically stable if :*

1. *all the roots of the characteristic equation for the first approximation system for (11) have negative real parts;*
2. $|R_i(t, u_1, u_2, ...u_{n(m+1)})| \leq \alpha \sum_{j=1}^{n(m+1)} |u_i|$, *where α is a sufficiently small constant, all $|u_i|$ are sufficiently small, i.e. $|u_i| \leq H$, where H is a sufficiently small positive constant and $t \geq t_0$.*

Theorem 3.2. *If at least one root of the characteristic equation has a positive real part, and condition (2) in Theorem 3.1 is satisfied, then the null solution of (11) is unstable.*

For the stability study of system (8) and (9), we will rewrite the system as:

$$\frac{d\mathrm{X}(t)}{dt} = \mathrm{K}_1[\mathrm{K}_2 - \mathrm{X}(t)] - \mathrm{K}_3\mathrm{V}(\mathrm{X}(t) - \mathrm{P}_{\mathrm{ICO}_2}), \tag{12}$$

$$\frac{d\mathrm{Y}(t)}{dt} = \mathrm{K}_4[\mathrm{K}_5 - \mathrm{K}_6\mathrm{Y}(t) - \mathrm{K}_7] + \mathrm{K}_8\mathrm{V}(\mathrm{P}_{\mathrm{IO}_2} - \mathrm{Y}(t)), \tag{13}$$

where

$$
\begin{aligned}
X(t) &= Pa_{CO_2}, \\
Y(t) &= Pa_{O_2}, \\
V &= \dot{V}_I(X(t-\tau), Y(t-\tau)), \\
\tau &= \tau_a, \\
K_1 &= 863\frac{\dot{Q}K_{CO_2}}{M_{L_{CO_2}}}, \\
K_2 &= P_{V_{CO_2}}, \\
K_3 &= \frac{E_F}{M_{L_{CO_2}}}, \\
K_4 &= 863\frac{\dot{Q}}{M_{L_{O_2}}}, \\
K_5 &= m_v P_{V_{O_2}} + B_v, \\
K_6 &= m_a, \\
K_7 &= B_a, \\
K_8 &= \frac{E_F}{M_{L_{O_2}}}.
\end{aligned}
$$

Note that V is increasing in $X(\cdot)$ and decreasing in $Y(\cdot)$. Simplifying these equations gives

$$\frac{dX(t)}{dt} = K_{11} - K_1 X(t) - K_3 V(X(t) - P_{I_{CO_2}}), \tag{14}$$

$$\frac{dY(t)}{dt} = K_{12} - K_{13} Y(t) + K_8 V(P_{I_{O_2}} - Y(t)), \tag{15}$$

where

$$
\begin{aligned}
K_{11} &= K_1 K_2, \\
K_{12} &= K_4 K_5 - K_7 K_4, \\
K_{13} &= K_4 K_6.
\end{aligned}
$$

Let

$$
\begin{aligned}
x(t) &= X(t) - P_{I_{CO_2}}, \\
y(t) &= P_{I_{O_2}} - Y(t),
\end{aligned}
$$

so that $x(t)$ represents the difference in inspired CO_2 and arterial CO_2 and $y(t)$ represents the difference in inspired O_2 and arterial O_2. We note that $P_{I_{CO_2}} \approx 0$. After some substitutions and simplifications, we obtain

$$\frac{dx(t)}{dt} = a_1 - a_2 x(t) - a_3 V x(t), \tag{16}$$

$$\frac{d\mathrm{y}(t)}{dt} = \mathrm{b}_1 - \mathrm{b}_2\mathrm{y}(t) - \mathrm{b}_3\mathrm{V}\mathrm{y}(t), \tag{17}$$

where

$$\begin{aligned}
\mathrm{a}_1 &= \mathrm{K}_{11} - \mathrm{K}_1\mathrm{P}_{\mathrm{I}_{\mathrm{CO}_2}},\\
\mathrm{a}_2 &= \mathrm{K}_1,\\
\mathrm{a}_3 &= \mathrm{K}_3,\\
\mathrm{b}_1 &= -\mathrm{K}_{12} + \mathrm{K}_{13}\mathrm{P}_{\mathrm{I}_{\mathrm{O}_2}},\\
\mathrm{b}_2 &= \mathrm{K}_{13},\\
\mathrm{b}_3 &= \mathrm{K}_8.
\end{aligned}$$

The $\mathrm{P}_{\mathrm{I}_{\mathrm{CO}_2}}$ level in ambient air is very small and we will assume that it is zero. It should be noted that the control function V has the following properties:

(i) $\mathrm{V} = \mathrm{V}(x(t-\tau), y(t-\tau))$, is now increasing in both x and y,
(ii) $\mathrm{V}(\mathrm{I}_\mathrm{P}, y) = 0$,
(iii) V is differentiable for $x \neq \mathrm{I}_\mathrm{P}$,
(iv) $\mathrm{V}_\mathrm{X} > 0$, $\mathrm{V}_\mathrm{y} > 0$, for $x > \mathrm{I}_\mathrm{P}$, $y > 0$.

The above system (16) and (17) is of the form

$$\dot{x}(t) = f(x_t).$$

where $f : C \to \mathbb{R}^2$ and $C = C([-r, 0], \mathbb{R}^2)$. $f(x_t)$ takes the form

$$f(x_t) = \begin{pmatrix} f_1(x_t) \\ f_2(x_t) \end{pmatrix}$$

and $x(t)$ takes the form $(x_1(t), x_2(t))$. We first observe the following:

Theorem 3.3. *The system (16) and (17) has a unique solution for $\sigma \in \mathbb{R}$ and $\phi \in C$.*

Proof. We will show that f is continuous on C and locally Lipschitz on compact sets of C. Recall that the norm on C is defined as follows. For $\phi \in C$,

$$|\phi|_\infty = \sup_{-r\le\theta\le 0} \sqrt{(\phi_1(\theta))^2 + (\phi_2(\theta))^2},$$

It is clear that if each f_i is continuous and locally Lipschitz, for $i = 1, 2$, then f is continuous and we can find a Lipschitz constant K for f.

Let $\vec{w} = (\vec{u}, \vec{v}) \in \mathbb{R}^2 \times \mathbb{R}^2$, where $\vec{u} = (u_1, u_2)$, $\vec{v} = (v_1, v_2)$ and with norm defined by $|(\vec{u}, \vec{v})|_{\mathbb{R}^2\times\mathbb{R}^2} = |\vec{u}|_{\mathbb{R}^2} + |\vec{v}|_{\mathbb{R}^2}$. Consider f_1 as a function defined on $\mathbb{R}^2 \times \mathbb{R}^2$ by

$$f_1(\vec{u}, \vec{v}) = \mathrm{a}_1 - \mathrm{a}_2 u_1 - \mathrm{a}_3\mathrm{V}(v_1, v_2)u_1, \tag{18}$$

where

$$\mathrm{V}(v_1, v_2) = \mathrm{G}_\mathrm{P}\exp(-0.05v_2)(v_1 - \mathrm{I}_\mathrm{P}).$$

Since $\mathbb{R}^2 \times \mathbb{R}^2 \cong \mathbb{R}^4$, it is clear that (18) is continuous on $\mathbb{R}^2 \times \mathbb{R}^2$. From now on $|\cdot|$ will represent the appropriate norm when no confusion will occur. Let $\phi = (\phi_1, \phi_2) \in C$ be chosen and let $\vec{w} = (\vec{u}, \vec{v}) \in \mathbb{R}^2 \times \mathbb{R}^2$ where $(\vec{u}, \vec{v})$ is defined as:

$$\vec{u} = \begin{pmatrix} u_1 \\ u_2 \end{pmatrix} = \begin{pmatrix} \phi_1(0) \\ \phi_2(0) \end{pmatrix}, \vec{v} = \begin{pmatrix} v_1 \\ v_2 \end{pmatrix} = \begin{pmatrix} \phi_1(-\tau) \\ \phi_2(-\tau) \end{pmatrix}.$$

Thus $\vec{w} = (\phi(0), \phi(-\tau))$ is a given element in $\mathbb{R}^2 \times \mathbb{R}^2$. Considering the right-hand side of (18) as a mapping on $\mathbb{R}^2 \times \mathbb{R}^2$, and for $\vec{w}$ defined above, for every $\epsilon = \epsilon(\vec{w}) > 0$ there is a $\delta > 0$ such that $|f_1(\vec{x}) - f_1(\vec{w})| < \epsilon$ when $|\vec{x} - \vec{w}| < \delta$. Let $|\phi - \psi| < \delta/2$ for $\psi \in C$. Then it follows that

$$|\phi(0) - \psi(0)| < \delta/2 \qquad \text{and} \qquad |\phi(-\tau) - \psi(-\tau)| < \delta/2.$$

For any ψ, let $\vec{x} = (\psi(0), \psi(-\tau))$. We have

$$|f_1(\psi) - f_1(\phi)| = |f_1(\vec{x}) - f_1(\vec{w})|$$

and

$$|f_1(\vec{x}) - f_1(\vec{w})| < \epsilon$$

when

$$\begin{aligned} |\vec{x} - \vec{w}| &= \sqrt{(\phi_1(0) - \psi_1(0))^2 + (\phi_2(0) - \psi_2(0))^2} \\ &\quad + \sqrt{(\phi_1(-\tau) - \psi_1(-\tau))^2 + (\phi_2(-\tau) - \psi_2(-\tau))^2} \\ &< \delta. \end{aligned}$$

That is, when $|\phi - \psi| < \delta/2$. We conclude that f_1 is continuous on C. A similar argument can be given for f_2 and thus f is continuous on C.

Again regarding f_1 as a mapping on $\mathbb{R}^2 \times \mathbb{R}^2$, it is clear that the exponential factor in V has continuous partial derivatives and will be locally Lipschitz on compact sets. Also, the second factor in V defined by the map $f : (\vec{u}, \vec{v}) \to [(v_1 - \mathrm{I_P})]$ is Lipschitz. Furthermore, sums and products of Lipschitz maps on compact sets will be Lipschitz. Therefore, the above mapping (18) will be locally Lipschitz on compact sets of $\mathbb{R}^2 \times \mathbb{R}^2$. Thus, if $\vec{x}, \vec{y} \in \mathbb{R}^2 \times \mathbb{R}^2$ are contained in a compact set, then there exists a $K > 0$ such that

$$|f_1(\vec{x}) - f_1(\vec{y})| < K|\vec{x} - \vec{y}|. \tag{19}$$

Now, let D be a compact set in C. Hence, for $\phi = (\phi_1, \phi_2) \in D$, we have $|\phi| < b$ for some $b > 0$. Thus the set $\{\phi(t) | \phi \in D, t \in [-r, 0]\}$ will be contained in the closed ball $B(0, b)$, a compact set in $\mathbb{R}^2$ and so pairs of the form $(\phi(0), \phi(-\tau))$ will be contained in the closed ball $B(0, 2b)$ in $\mathbb{R}^2 \times \mathbb{R}^2$. This ball is compact and f_1 will be Lipschitz on $B(0, 2b)$ with Lipschitz constant K. Consider, for $\phi,\ \psi \in D$,

$$\begin{aligned} f_1(\phi) - f_1(\psi) = &-\mathrm{a}_2(\phi_1(0) - \psi_1(0)) \\ &-\mathrm{a}_3(\mathrm{V}(\phi_1(-\tau), \phi_2(-\tau))\phi_1(0) - \mathrm{V}(\psi_1(-\tau), \psi_2(-\tau))\psi_1(0)). \end{aligned}$$

Again considering the right-hand side of (18) as a mapping from $\mathbb{R}^2 \times \mathbb{R}^2$, and making the identification

$$\begin{pmatrix} u_1 \\ u_2 \end{pmatrix} = \begin{pmatrix} \phi_1(0) \\ \phi_2(0) \end{pmatrix}, \begin{pmatrix} v_1 \\ v_2 \end{pmatrix} = \begin{pmatrix} \phi_1(-\tau) \\ \phi_2(-\tau) \end{pmatrix},$$

(similarly for ψ) we have

$$\begin{aligned} |f_1(\phi) - f_1(\psi)| < K\sqrt{(\phi_1(0) - \psi_1(0))^2 + (\phi_2(0) - \psi_2(0))^2} \\ + K\sqrt{(\phi_1(-\tau) - \psi_1(-\tau))^2 + (\phi_2(-\tau) - \psi_2(-\tau))^2} \\ < 2K|\phi - \psi|. \end{aligned}$$

Thus f_1 is locally Lipschitz on compact sets. A similar argument can be given for f_2 and thus f is locally Lipschitz. From well known results (see, e.g., [14] Theorems (2.2.1) and (2.2.3)) it follows that the system (16) and (17) has a unique solution for $\sigma \in \mathbb{R}$ and $\phi \in C$. This ends the proof. □

Note that by introducing added components to the product space $\mathbb{R}^2 \times \mathbb{R}^2$ to account for the brain transport delay and tissue transport delays, we can establish the same results for the five-dimensional state space model presented in Section 2. We further note that from Theorem 2.2.2 in [14] we are also guaranteed that the solutions are continuously dependent on initial data so that the models are well-posed.

We now will show that the system (16) and (17) has a unique positive equilibrium.

Theorem 3.4. *The above system (16) and (17) has a unique positive equilibrium* $(\bar{x}, \bar{y})$ *where* $\bar{x} > I_P$ *and* $\bar{y} > 0$.

Proof. The equilibrium solution $(\bar{x}, \bar{y})$ satisfies

$$0 = a_1 - a_2\bar{x} - a_3\bar{V}\bar{x}, \tag{20}$$

$$0 = b_1 - b_2\bar{y} - b_3\bar{V}\bar{y}, \tag{21}$$

where $\bar{V} = V(\bar{x}, \bar{y})$. Note that $\frac{a_1}{a_2} = P_{V_{CO_2}}$ and will always be physiologically much larger than I_P, the threshold level for zero ventilation. This implies that $\bar{V} = 0$ is impossible at equilibrium. For then, $\bar{V} = 0 \Rightarrow \bar{x} \le I_P$ but $\bar{V} = 0 \Rightarrow \bar{x} = \frac{a_1}{a_2}$ from solving (20) for $\bar{x}$ and this contradicts that $\frac{a_1}{a_2} >> I_P$. Now (20) gives

$$\bar{x} = \frac{a_1}{a_2 + a_3\bar{V}} \tag{22}$$

and (21) implies

$$\bar{V} = \frac{b_1}{b_3\bar{y}} - \frac{b_2}{b_3}. \tag{23}$$

Note that this equation gives the value for $\bar{V}$ at equilibrium and is not meant as a formula for $\bar{V}$ in terms of $\bar{y}$. Substituting (23) into (22) gives

$$\bar{x} = \frac{a_1}{a_2 + a_3(\frac{b_1}{b_3\bar{y}} - \frac{b_2}{b_3})}. \tag{24}$$

At equilibrium, $\bar{y} \geq \frac{b_1}{b_2} \Leftrightarrow \bar{V} \leq 0$. This is impossible at equilibrium so that $\bar{y} < \frac{b_1}{b_2}$. Now using (24), we see that $\bar{x} = x(\bar{y})$ is monotonically increasing in $\bar{y}$ and $\bar{x} \to 0$ monotonically as $\bar{y} \to 0$. Thus we may find a unique $\bar{y}$ such that $\bar{x}$ is as close to (but greater than) $\bar{x} = I_P$ as we wish. Furthermore, from the equation for V we may bound the exponential factor involving y on the interval $0 < y < \frac{b_1}{b_2}$ by a positive value M. Thus

$$V \leq M(x - I_P).$$

We can choose $\bar{x}$ so that V is as small as we wish and find a corresponding $\bar{y}$ using (24). We also note that

$$g(y) = \frac{b_1}{b_3 y} - \frac{b_2}{b_3}$$

is decreasing in $\bar{y}$. By choosing $\bar{x}$ sufficiently close to x= I_P (call it $\bar{x}_{I_P}$) we can find a pair $(\bar{x}_{I_P}, \bar{y}_{I_P})$ so that

$$\bar{V}(\bar{x}_{I_P}, \bar{y}_{I_P}) < g(\bar{y}_{I_P}) \tag{25}$$

where $\bar{y}_{I_P} < \frac{b_1}{b_2}$.

Now V is monotonically increasing in x and y and $\bar{x} = x(\bar{y})$ is monotonically increasing in $\bar{y}$ from (24). Thus $\bar{V}(\bar{x}(\bar{y}), \bar{y})$ is increasing in $\bar{y}$ where $\bar{y}_{I_P} < \frac{b_1}{b_2}$. Also $g(y) = \frac{b_1}{b_3 y} - \frac{b_2}{b_3}$ is decreasing in y and $g(\frac{b_1}{b_2}) = 0$. Thus if we begin with the relation (25) there will be a unique solution $\bar{y}^*$ of

$$\bar{V}(\bar{x}(\bar{y}), \bar{y}) = \frac{b_1}{b_3\bar{y}} - \frac{b_2}{b_3}$$

where $\bar{y}_{I_P} < \bar{y}^* < \frac{b_1}{b_2}$. Using the solution $\bar{y}^*$ to define $\bar{x}^*$ we get upon substituting $\bar{y}^*$ into (24) the corresponding uniquely defined $\bar{x}^*$:

$$\bar{x}^* = \frac{a_1}{a_2 + a_3(\frac{b_1}{b_3\bar{y}^*} - \frac{b_2}{b_3})}.$$

Note that $I_P < \bar{x}^* < \frac{a_1}{a_2}$. Solving for $\bar{V}$ in (20) at equilibrium we see that

$$\bar{V} = \frac{a_1}{a_3\bar{x}} - \frac{a_2}{a_3} \tag{26}$$

and substituting $\bar{x}^*$ defined above we get

$$\bar{V}(\bar{x}^*(\bar{y}^*), \bar{y}^*) = \frac{a_1}{a_3\left(\frac{a_1}{a_2+a_3(\frac{b_1}{b_3}\bar{y}^*-\frac{b_2}{b_3})}\right)} - \frac{a_2}{a_3} = \frac{b_1}{b_3\bar{y}^*} - \frac{b_2}{b_3}.$$

Thus $\bar{V}$ as defined by (23) and (26) are equal at $(\bar{x}^*, \bar{y}^*)$ and so $(\bar{x}^*, \bar{y}^*)$ is indeed a positive equilibrium and is unique by the above argument. This completes our proof. □

We will now consider the stability of the above nonlinear system of delay differential equations (16) and (17). Let

$$\xi(t) = x(t) - \bar{x},$$
$$\eta(t) = y(t) - \bar{y}.$$

The linearized system of (16) and (17) is given by

$$\frac{d\xi(t)}{dt} = (-a_2 - a_3\bar{V})\xi(t) - a_3\bar{x}\bar{V}_x\xi(t-\tau) - a_3\bar{x}\bar{V}_y\eta(t-\tau), \tag{27}$$

$$\frac{d\eta(t)}{dt} = (-b_2 - b_3\bar{V})\eta(t) - b_3\bar{y}\bar{V}_x\xi(t-\tau) - b_3\bar{y}\bar{V}_y\eta(t-\tau). \tag{28}$$

Writing in matrix form

$$\frac{d}{dt}\begin{pmatrix}\xi(t)\\ \eta(t)\end{pmatrix} = A\begin{pmatrix}\xi(t)\\ \eta(t)\end{pmatrix} + B\begin{pmatrix}\xi(t-\tau)\\ \eta(t-\tau)\end{pmatrix},$$

where

$$A = \begin{pmatrix}-a_2 - a_3\bar{V} & 0\\ 0 & -b_2 - b_3\bar{V}\end{pmatrix}, \quad B = \begin{pmatrix}-a_3\bar{x}\bar{V}_x & -a_3\bar{x}\bar{V}_y\\ -b_3\bar{y}\bar{V}_x & -b_3\bar{y}\bar{V}_y\end{pmatrix}.$$

The characteristic equation is

$$\det(\lambda I - A - Be^{-\tau\lambda})_{2x2} = 0. \tag{29}$$

Upon substituting the matrix A and B we get

$$\det\begin{pmatrix}\lambda + (a_2 + a_3\bar{V}) + a_3\bar{x}\bar{V}_x e^{-\tau\lambda} & a_3\bar{x}\bar{V}_y e^{-\tau\lambda}\\ b_3\bar{y}\bar{V}_x\, e^{-\tau\lambda} & \lambda + (b_2 + b_3\bar{V}) + b_3\bar{y}\bar{V}_y e^{-\tau\lambda}\end{pmatrix} = 0.$$

Expanding this determinant gives

$$\Delta(\lambda, \tau) = P(\lambda) + Q(\lambda)e^{-\tau\lambda} = 0 \tag{30}$$

where

$$P(\lambda) = \lambda^2 + (b_2 + b_3\bar{V} + a_2 + a_3\bar{V})\lambda + (a_2 + a_3\bar{V})(b_2 + b_3\bar{V}) \tag{31}$$

and

$$Q(\lambda) = [(b_3\bar{y}\bar{V}_y + a_3\bar{x}\bar{V}_x)\lambda + (a_2 + a_3\bar{V})b_3\bar{y}\bar{V}_y + (b_2 + b_3\bar{V})a_3\bar{x}\bar{V}_x)]. \tag{32}$$

Notice that

$$\begin{aligned}\Delta(\lambda, 0) = \lambda^2 &+ (b_2 + b_3\bar{V} + a_2 + a_3\bar{V} + b_3\bar{y}\bar{V}_y + a_3\bar{x}\bar{V}_x)\lambda \\ &+ (a_2 + a_3\bar{V})(b_2 + b_3\bar{V}) + (a_2 + a_3\bar{V})b_3\bar{y}\bar{V}_y \\ &+ (b_2 + b_3\bar{V})a_3\bar{x}\bar{V}_x\end{aligned} \tag{33}$$

has all positive coefficients so that the roots to the characteristic equation have negative real parts when no delay is present. Also

$$\begin{aligned}\Delta(0, \tau) = &(a_2 + a_3\bar{V})(b_2 + b_3\bar{V}) \\ &+ (a_2 + a_3\bar{V})b_3\bar{y}\bar{V}_y + a_3\bar{x}\bar{V}_x(b_2 + b_3\bar{V}) \neq 0.\end{aligned} \tag{34}$$

To simplify subsequent calculations we will use the following notation:

$$\begin{aligned}A_1 &= a_2 + a_3\bar{V}, \\ A_2 &= a_3\bar{x}\bar{V}_x, \\ B_1 &= b_2 + b_3\bar{V}, \\ B_2 &= b_3\bar{y}\bar{V}_y.\end{aligned}$$

In the simpler model analyzed by Cooke and Turi [5] they developed stability criteria based on the relation between the value $\bar{V}$ and the value $\bar{x}\bar{V}_x + \bar{y}\bar{V}_y$. We will find that in our model the situation is more complicated. We establish the following lemmas which will be needed to analyze the stability properties of the above system (27) and (28).

Lemma 3.1. *If* $\bar{V} \geq \bar{x}\bar{V}_x + \bar{y}\bar{V}_y$ *then* $\Delta(i\omega, \tau) \neq 0$ *for* $\omega \in R/\{0\}, \tau \geq 0$.

Proof. As noted above $\Delta(0, \tau) \neq 0$. Also for $\omega \in R$, we have

$$|P(i\omega)|^2 - |Q(i\omega)|^2 = \omega^4 + k_1\omega^2 + k_2 \tag{35}$$

where

$$\begin{aligned}k_1 &= A_1^2 + B_1^2 - (A_2 + B_2)^2, \\ k_2 &= A_1^2B_1^2 - (A_1B_2 + A_2B_1)^2.\end{aligned}$$

Consider

$$\begin{aligned}A_1B_1 - (A_1B_2 + A_2B_1) = &(a_2 + a_3\bar{V})(b_2 + b_3\bar{V}) \\ &-[(a_2 + a_3\bar{V})b_3\bar{y}\bar{V}_y + (b_2 + b_3\bar{V})a_3\bar{x}\bar{V}_x].\end{aligned} \tag{36}$$

If $\bar{V} \geq \bar{x}\bar{V}_X + \bar{y}\bar{V}_Y$ and $a_2 = 0 = b_2$, then

$$\begin{aligned} A_1B_1 - (A_1B_2 + A_2B_1) &= a_3\bar{V}b_3\bar{V} - (a_3\bar{V}b_3\bar{y}\bar{V}_Y + b_3\bar{V}a_3\bar{x}\bar{V}_X) \\ &= a_3b_3\bar{V}(\bar{V} - (\bar{y}\bar{V}_Y + \bar{x}\bar{V}_X)) \geq 0. \end{aligned} \tag{37}$$

Also given $\bar{V} \geq \bar{x}\bar{V}_X + \bar{y}\bar{V}_Y$ it follows that

$$b_2a_3\bar{V} > b_2a_3\bar{x}\bar{V}_X \quad \text{and} \quad a_2b_3\bar{V} > a_2b_3\bar{y}\bar{V}_Y. \tag{38}$$

Now, as a_2 increases, the first term on the right hand side of (36) increases by $a_2b_2 + a_2b_3\bar{V}$ while the second term increases by $a_2b_3\bar{y}\bar{V}_Y$. From inequality (38) we see that the first term is larger than the second so that (37) still holds for non-negative a_2. The same is true as b_2 increases. Therefore, for $a_2 \geq 0$, $b_2 \geq 0$, we have that

$$A_1B_1 - (A_1B_2 + A_2B_1) \geq 0.$$

This implies that

$$k_2 = A_1^2B_1^2 - (A_1B_2 + A_2B_1)^2 \geq 0.$$

Also, if $\bar{V} \geq \bar{x}\bar{V}_X + \bar{y}\bar{V}_Y$ and $a_2 = 0 = b_2$, then

$$\begin{aligned} A_1^2 + B_1^2 &= (a_3^2 + b_3^2)\bar{V}^2 \geq (a_3^2 + b_3^2)(\bar{x}\bar{V}_X + \bar{y}\bar{V}_Y)^2 \\ &= (a_3^2 + b_3^2)(\bar{x}^2\bar{V}_X^2 + 2\bar{x}\bar{y}\bar{V}_X\bar{V}_Y + \bar{y}^2\bar{V}_Y^2) \\ &= a_3^2\bar{x}^2\bar{V}_X^2 + (a_3^2 + b_3^2)(2\bar{x}\bar{y}\bar{V}_X\bar{V}_Y) + a_3^2\bar{y}^2\bar{V}_Y^2 + b_3^2\bar{x}^2\bar{V}_X^2 + b_3^2\bar{y}^2\bar{V}_Y^2) \\ &> a_3^2\bar{x}^2\bar{V}_X^2 + 2a_3b_3\bar{x}\bar{y}\bar{V}_X\bar{V}_Y + b_3^2\bar{y}^2\bar{V}_Y^2 \\ &= (a_3\bar{x}\bar{V}_X + b_3\bar{y}\bar{V}_Y)^2 \\ &= (A_2 + B_2)^2 \end{aligned}$$

where we have used $(a_3^2+b_3^2) \geq 2a_3b_3 \geq a_3b_3$ since a_3 and b_3 are positive constants. So we have

$$A_1^2 + B_1^2 - (A_2 + B_2)^2 > 0.$$

Since only A_1 and B_1 increase as a_2 and b_2 increase it follows that

$$A_1^2 + B_1^2 > (A_2 + B_2)^2$$

for a_2 and b_2 positive constants. Thus $k_1 > 0$ and

$$|P(i\omega)|^2 - |Q(i\omega)|^2 = \omega^4 + k_1\omega^2 + k_2 \neq 0 \ \text{ for } \omega \in R/\{0\}.$$

This implies

$$(|P(i\omega)| - |Q(i\omega)|)(|P(i\omega)| + |Q(i\omega)|) \neq 0.$$

Thus

$$|P(i\omega)| - |Q(i\omega)| \neq 0.$$

This gives

$$|\Delta(i\omega,\tau)| \geq ||\mathrm{P}(i\omega)| - |\mathrm{Q}(i\omega)|| > 0.$$

Hence,

$$\Delta(i\omega,\tau) = \mathrm{P}(i\omega) + \mathrm{Q}(i\omega)e^{-\tau i\omega} \neq 0,\ \ \omega \in R/\{0\} \quad , \tau \geq 0.$$

This ends the proof. □

When $\bar{\mathrm{V}} < \bar{\mathrm{x}}\bar{\mathrm{V}}_{\mathrm{X}} + \bar{\mathrm{y}}\bar{\mathrm{V}}_{\mathrm{Y}}$ the conditions which determine the signs of k_1 and k_2 are not so transparent and we will consider several cases.

Lemma 3.2. *IF $A_1B_1 < A_1B_2 + A_2B_1$ then there is a unique pair of ω_o, τ_o with $\omega_o > 0$, $\tau_o > 0$, and $\omega_o\tau_o < 2\pi$ such that $\Delta(i\omega_o, \tau_o) = 0$.*

Proof. If $\mathrm{A}_1\mathrm{B}_1 - (\mathrm{A}_1\mathrm{B}_2 + \mathrm{A}_2\mathrm{B}_1) < 0$ or equivalently $\mathrm{k}_2 < 0$, we have that

$$|\mathrm{P}(i\omega)|^2 - |\mathrm{Q}(i\omega)|^2 = \omega^4 + \mathrm{k}_1\omega^2 + \mathrm{k}_2 = v^2 + \mathrm{k}_1 v + \mathrm{k}_2 = \hat{F}(v)$$

where $v = \omega^2$. Then $\hat{F}(v)$ has a unique positive root $v = v_o$

$$v_o = 1/2(-\mathrm{k}_1 + \sqrt{\mathrm{k}_1^2 - 4\mathrm{k}_2}) > 0.$$

Thus

$$|\mathrm{P}(i\omega)|^2 - |\mathrm{Q}(i\omega)|^2 = 0$$

if and only if $\omega = \pm\omega_o$ where $\omega_o = \sqrt{v_o} \in R$. The condition

$$|\mathrm{P}(i\omega_o)|^2 - |\mathrm{Q}(i\omega_o)|^2 = 0$$

implies that

$$|\mathrm{P}(i\omega_o)| = |\mathrm{Q}(i\omega_o)|$$

and thus $\frac{\mathrm{P}(i\omega_o)}{\mathrm{Q}(i\omega_o)}$ lies on the unit circle. Note that $|\mathrm{Q}(i\omega_o)| \neq 0$ since it is linear with real coefficients. This means that there exist a unique τ_o such that $\tau_o > 0$, $\omega_o > 0$, $\tau_o\omega_o < 2\pi$ and

$$e^{-i\tau_o\omega_o} = -\frac{\mathrm{P}(i\omega_o)}{\mathrm{Q}(i\omega_o)}. \tag{39}$$

Consequently, $\tau_n = \tau_o + \frac{2n\pi}{\omega_o}, \quad n = 0, 1, 2, ...,$ also satisfies

$$e^{-i\tau_n\omega_o} = -\frac{\mathrm{P}(i\omega_o)}{\mathrm{Q}(i\omega_o)}. \tag{40}$$

Thus the characteristic equation

$$\Delta(z,\tau) = \mathrm{P}(z) + \mathrm{Q}(z)e^{-\tau z} = 0$$

has conjugate pairs of imaginary roots $\omega\tau_n$ where

$$\omega = \pm\omega_o \quad \text{and} \quad \tau_n = \tau_o + \frac{2n\pi}{\omega_o} \quad n = 0, 1, 2, ... \tag{41}$$

and a unique positive pair τ_o, ω_o where $\tau_o\omega_o < 2\pi$. This completes the proof. □

Lemma 3.3. *IF $A_1B_1 \geq A_1B_2 + A_2B_1$ then the following is true:*

1. *If $A_1B_1 = A_1B_2 + A_2B_1$ then there is at most a unique pair of ω_o, τ_o with $\omega_o > 0$, $\tau_o > 0$, $\omega_o\tau_o < 2\pi$ such that $\Delta(i\omega_o, \tau_o) = 0$.*
2. *If $A_1B_1 > A_1B_2 + A_2B_1$ then there are at most two pairs of ω_i, τ_i with $\omega_i > 0$, $\tau_i > 0$, and $\omega_i\tau_i < 2\pi$ for $i = 1, 2$.*

Proof. (1) If $\mathrm{A_1B_1 = A_1B_2 + A_2B_1}$ so that $\mathrm{k_2} = 0$ then

$$|\mathrm{P}(i\omega)|^2 - |\mathrm{Q}(i\omega)|^2 = \omega^4 + \mathrm{k_1}\omega^2 + \mathrm{k_2} = v(v + \mathrm{k_1}) = \hat{F}(v)$$

which has at most one positive solution if $\mathrm{k_1} < 0$. Statement (1) follows from using similar arguments as in Lemma 3.1.
(2) If $\mathrm{A_1B_1 > A_1B_2 + A_2B_1}$ so that $\mathrm{k_2} > 0$ then

$$\omega^4 + \mathrm{k_1}\omega^2 + \mathrm{k_2} = v^2 + \mathrm{k_1}v + \mathrm{k_2} = 0$$

will have no positive root if $\mathrm{k_1} \geq 0$ and two positive roots if $\mathrm{k_1} < 0$ and $\mathrm{k_1^2} - 4\mathrm{k_2} > 0$. Again the conclusions about ω and τ follow as above. This ends the proof. □

Notice that the condition $\mathrm{A_1B_1 > A_1B_2 + A_2B_1}$ and its variations reflects physiological considerations. The parameters $\mathrm{a_2}$, $\mathrm{b_2}$ are linear functions of $\dot{\mathrm{Q}}$ (they depend on compartment volumes also) so that $\mathrm{A_1B_1}$ varies with $\mathrm{o}(\dot{\mathrm{Q}}^2)$ while $\mathrm{A_1B_2+A_2B_1}$ varies with $\mathrm{o}(\dot{\mathrm{Q}})$. $\mathrm{k_2}$ will cross to nonnegative values for $\mathrm{a_2}$, $\mathrm{b_2}$ sufficiently large (assuming $\bar{\mathrm{V}}$, $\bar{\mathrm{V}}_\mathrm{X}$ and $\bar{\mathrm{V}}_\mathrm{y}$ are fixed). The above condition reflects the interaction of $\dot{\mathrm{Q}}$, $\bar{\mathrm{V}}$, $\bar{\mathrm{V}}_\mathrm{X}$ and $\bar{\mathrm{V}}_\mathrm{y}$ and $\mathrm{G_P}$. Steady state values do change as $\mathrm{G_P}$ and $\dot{\mathrm{Q}}$ change but larger values for $\dot{\mathrm{Q}}$ (together with reasonable assumptions on other parameters) does move the system into more stable configurations. Larger $\mathrm{G_P}$ values, on the other hand, tend to destabilize the system. The parameter values reflected in $\mathrm{a_3}$ and $\mathrm{b_3}$ correspond to compartment volumes and the respiratory efficiency factor $\mathrm{E_F}$ which mimics the effects of dead space ventilation and diffusion inefficiencies. In the two-dimensional model manipulating $\mathrm{E_F}$ acts to change controller gain. The factors we can manipulate are $\mathrm{G_P}$, $\dot{\mathrm{Q}}$, compartment volumes and $\mathrm{E_F}$. We refer the reader simulation studies in Section 3.3 for additional discussion.

Before we state the main results of this section which give stability results in terms of the delay variable τ, we recall the following theorem that originally is due to Cooke and van den Driessche [5]. The version given below is a corrected version proposed by Boese [2] (see also Theorem 4.1 on page 83 in [18]). Let the general characteristic equation to a linear system of differential equations with one delay be given as

$$\Delta(z, \tau) = \mathrm{P}(z) + \mathrm{Q}(z)e^{-\tau z} = 0. \tag{42}$$

Theorem 3.5. *Consider (42) where P and Q are analytic functions in a right half plane Re$z > -\delta$, $\delta > 0$ which satisfies the following conditions*

(i) *$P(z)$ and $Q(z)$ have no common imaginary zeroes;*
(ii) $\overline{P(-iy)} = P(iy)$, $\overline{Q(-iy)} = Q(iy)$ *for real y;*
(iii) $P(0) + Q(0) \neq 0$;

(iv) lim sup$\{|Q(\lambda)/P(\lambda)| : |\lambda| \to \infty, Re\lambda \geq 0\} < 1$*;*
(v) $F(y) = |P(iy)|^2 - |Q(iy)|^2$ *has at most a finite number of real zeroes.*

Then the following statements are true.

1. *If* $F(y) = 0$ *has no positive roots then if (42) is stable at* $\tau = 0$ *it remains stable for all* $\tau \geq 0$*. If (42) is unstable for* $\tau = 0$ *then it remains unstable for* $\tau \geq 0$*.*
2. *If* $F(y) = 0$ *has at least one positive root and each such root is simple then as* τ *increases stability switches may occur. There exists a positive number* τ^* *such that (42) is unstable for all* $\tau > \tau^*$*. As* τ *varies from 0 to* τ^* *at most a finite number of stability switches occur.*

The proof of this theorem is given in the above cited paper. The idea behind the theorem is that roots of

$$\Delta(z, \tau) = \mathrm{P}(z) + \mathrm{Q}(z)e^{-\tau z} = 0$$

vary continuously with τ. We may consider a root of the characteristic equation to be a function of τ in the sense that a small change in the parameter τ produces a small change in any root to the characteristic equation. We write $z = z(\tau)$. The justification for this follows from Rouche's Theorem and a proof may be found in [8]. Thus if there exists a τ_1 for which all roots have negative real part and a $\tau_2 > \tau_1$ for which there are roots with positive real part then there must be a τ^* such that $\tau_1 < \tau^* < \tau_2$ for which there is an imaginary root to (42). Informally, we say that if a root crosses from the negative complex half plane to the positive half plane as τ increases then for some τ^* there must be a crossover point on the imaginary axis, i.e. an imaginary root iy_{τ^*} to the characteristic equation for that τ^*.

The equation $F(y) = 0$ is used to find the crossover points on the imaginary axis. Without loss of generality, we consider $y > 0$. It is established in the proof of Theorem 3.5 that the statement that y is a simple root of $F(y) = 0$ is equivalent to the statement that there are an infinite number of τ^* for which iy is a root of (42) and for each such τ^* we have that iy is a simple root of (42). We denote this relation between iy and τ^* by iy_{τ^*}. Now, if a positive root y of $F(y) = 0$ is simple, we may apply the Inverse Function Theorem for complex variables using this simple imaginary root iy and τ^* (42). Using this theorem, we may actually solve for roots z in terms of τ in a neighborhood of a τ^* for which iy_{τ^*} is a simple root of (42). Furthermore, $z = z(\tau)$ will be differentiable (with derivative $z'(\tau) \neq 0$) at τ^*.

It can further be shown that, at such roots y of $F(y) = 0$ and τ^* for which iy_{τ^*} is a simple root of (42), the *sign*$\{\mathrm{Re}\ z'(\tau)|_{\tau^*}\} =$ *sign*$\{F'(y)|_{y_{\tau^*}}\}$. Thus the change in the real part of the roots can be calculated and it can be determined whether roots move from the left half plane to the right half plane as τ varies through τ^*. That is, the crossing direction of the roots can be ascertained. Note also that from the above equation we see that the *sign*$\{\mathrm{Re}\ z'(\tau)|_{\tau^*}\}$ is independent of τ^* at these simple imaginary roots. If there is only one simple root y to $F(y) = 0$ and $z'(\tau) > 0$ for this iy_{τ^*} then roots may only cross from the negative to the positive half plane.

Furthermore, if P and Q are polynomials with real coefficients where n is the degree of P, m is the degree of Q and $n > m$, then $F(y)$ is an even polynomial of degree 2n. By setting $x = y^2$, $y > 0$, we define a new function $\hat{F}(x)$ which will be a polynomial of degree n. $\hat{F}(x)$ can be factored as

$$\hat{F}(x) = \prod_{j=1}^{n}(x - r_j).$$

In the following corollary it is shown how the crossing directions may be calculated in this case.

Corollary 3.1. *If P and Q are polynomials with real coefficients where n is the degree of P, m is the degree of Q and $n > m$ and where $r_1 > r_2 > r_3 > ... > r_p > 0$ are the distinct roots of $\hat{F}(x)$, then $\pm i y_k = \pm\sqrt{r_k}(k = 1, 2, ..., p)$ are the possible roots of (42) on the imaginary axis. Assume that these roots are simple. Then the crossing direction s_k at $i y_k$ is given by*

$$s_k = sign\{\prod_{\substack{j=1 \\ j \neq k}}^{p}(r_k - r_j)\}.$$

If there is only one root y then the sign must be positive so that roots may only cross from the negative to positive half plane. We are thus led to the following:

Theorem 3.6. *For the above defined system (16) and (17), if $\bar{V} \geq \bar{x}\bar{V}_X + \bar{y}\bar{V}_Y$ then the equilibrium $(\bar{x}, \bar{y})$ is asymptotically stable for all $\tau \geq 0$.*

Proof. This result follows from Lemma 3.1, and Theorem 3.5. We note that P and Q for our system satisfy the conditions (i), (ii) (iv) and (v) required by Theorem 3.5 since they are polynomials with real coefficients and can have no common imaginary root since Q is linear. Also as noted above, (33) establishes that, for $\tau = 0$, all roots of $\Delta(\lambda, 0) = 0$ have negative real part so that the system is stable at $\tau = 0$. (34) established that $\Delta(0, \tau) \neq 0$ so that (iii) is satisfied. Lemma 3.1 establishes that there is no positive root to (35). Hence the result follows from conclusion 1 in Theorem 3.5. Note that all the roots ω_o in the above lemmas are simple. This ends the proof. □

Using the results from (3.1) and (3.5) we have:

Theorem 3.7. *For the above defined system, (16) and (17), if $A_1 B_1 - (A_1 B_2 + A_2 B_1) < 0$ then there exists a $\tau^* > 0$ such that the equilibrium $(\bar{x}, \bar{y})$ is asymptotically stable for $\tau < \tau^*$ and unstable for $\tau > \tau^*$.*

Proof. This result follows immediately from Lemma 3.2, conclusion 2 in Theorem 3.5, Corollary 3.1 and the comments in Theorem 3.6. The crossing direction is guaranteed to be from the negative to positive half plane as there is only one simple root. This ends the proof. □

We may find τ^* by solving (35) for ω and then solving for τ^* in equation (39). That is, τ^* is a solution to

$$e^{-\tau^* i\omega_o} = -\frac{\mathrm{P}(i\omega_o)}{\mathrm{Q}(i\omega_o)}$$

and τ^* is such that $\omega_o \tau^* < 2\pi$.

Theorem 3.8. *For the above defined system (16) and (17), if* $A_1B_1 - (A_1B_2 + A_2B_1) > 0$ *and* $A_1^2 + B_1^2 - (A_2 + B_2)^2 = k_1 > 0$ *then the equilibrium* $(\bar{x}, \bar{y})$ *is asymptotically stable for all* $\tau \geq 0$.

Proof. This follows exactly as in Theorem 3.6. □

We point out here that similar results may be stated for the other conditions in Lemma 3.3 but numerical studies indicate that $k_1 > 0$ will not occur given reasonable physiological values for the parameters unless $k_2 > 0$ so that we will not consider these cases. Even should this condition be satisfied we see that the system will eventually become unstable after a finite number of stability switches (there are then at most two positive roots). From a physiological perspective, later switches will require delay times probably too long to be physiologically meaningful. Two numerical studies are included in section 3.5 below indicating the relationships between k_1 and k_2 for various parameter values.

3.3. *Numerical simulation studies*

In this section, numerical simulations on the simplified two-dimensional state space model described in Section 3.1 were carried out to verify the stability analysis presented in Section 3.2. All steady state and stability calculations were done using Maple 5 release 3. In addition, the initial conditions are chosen to be small offsets from the steady state values. We plot Pa_{CO_2}, Pa_{O_2}, and ventilation rate denoted by Ve.

Table 1 (and other tables) gives the steady state values for $\bar{x}$, $\bar{y}$, $\bar{x}\bar{V}_X + \bar{y}\bar{V}_Y$, G_P, $\dot{Q}$, $\bar{V}$, k_2 and k_2 (where appropriate). All tables are found at the end of the paper. The table also gives the natural delay time τ_{norm} as defined by the vascular volumes and $\dot{Q}$ and $\dot{Q}_B$ as well as a τ^* multiplier for τ_{norm} which indicates when instability sets in. The τ^* multiplier describes by what factor the normal delay τ_{norm} must be increased to produce instability in the system. Figure 3 shows simulation results for a moderate controller gain and $\tau < \tau^*$. Figure 4 represents the situation when $\tau > \tau^*$.

Figure 5 gives the simulation results for a larger controller gain G_P and $\tau < \tau^*$. Figure 6 represents the situation when $\tau > \tau^*$.

The parameter values and stability calculations for Figures 5 and 6 are given in Table 2. We note that parameters in Table 2 are such that $A_1^2B_1^2 - (A_2B_1 + A_1B_2)^2 << 0$ and $\bar{V} << \bar{x}\bar{V}_X + \bar{y}\bar{V}_Y$ than was the case in Figures 3 and 4 so that the system will have delay related instability for all parameter values in the physiological range. The ratio $\frac{\tau^*}{\tau_{norm}}$ is approximately 2:1 which is much lower than is to be expected in real individuals. However, we are only modeling the peripheral control system which, it is believed, is responsible for the unstable phenomena in respiratory physiology. Thus, the model supports this idea.

We see that larger controller gain produces a smaller τ^* indicating that the controller gain level is important for stability properties. One reason that the peripheral controller contributes so much to instability characteristics is that it responds to Pa_{CO_2} and Pa_{O_2} which (as can be seen in the five-dimensional model simulations, Figure 2) varies much more than the other state variables. Also, it is known that

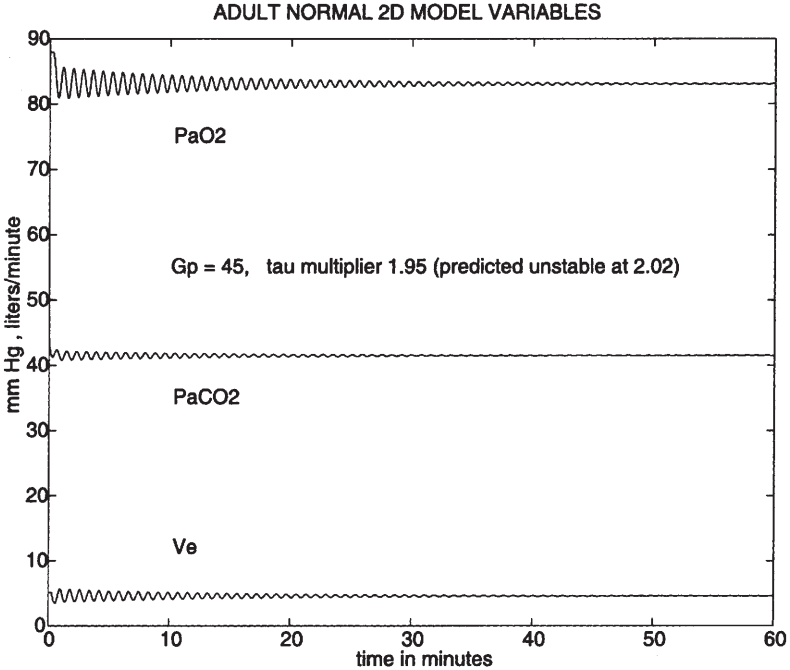

Fig. 3. Stable two-dimensional basic model with moderate gain.

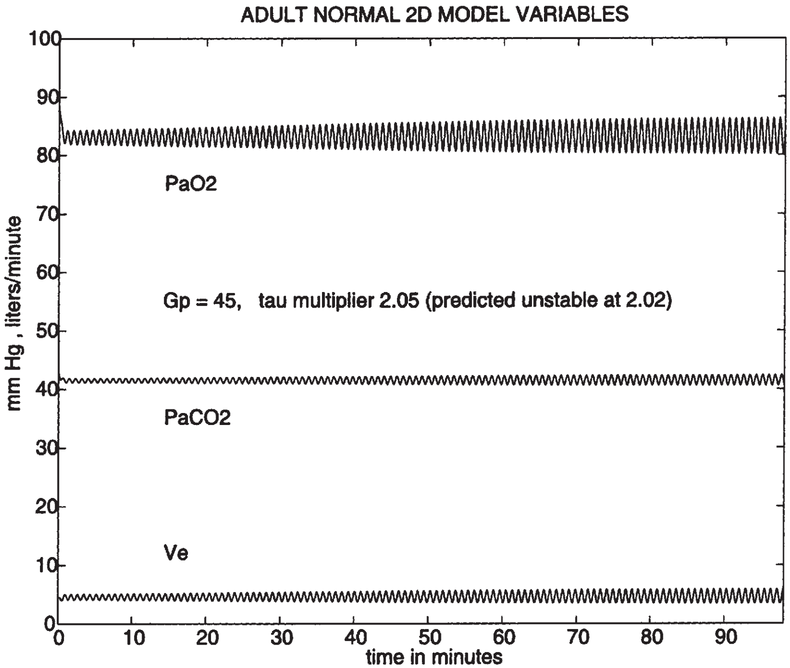

Fig. 4. Unstable two-dimensional basic model with moderate gain.

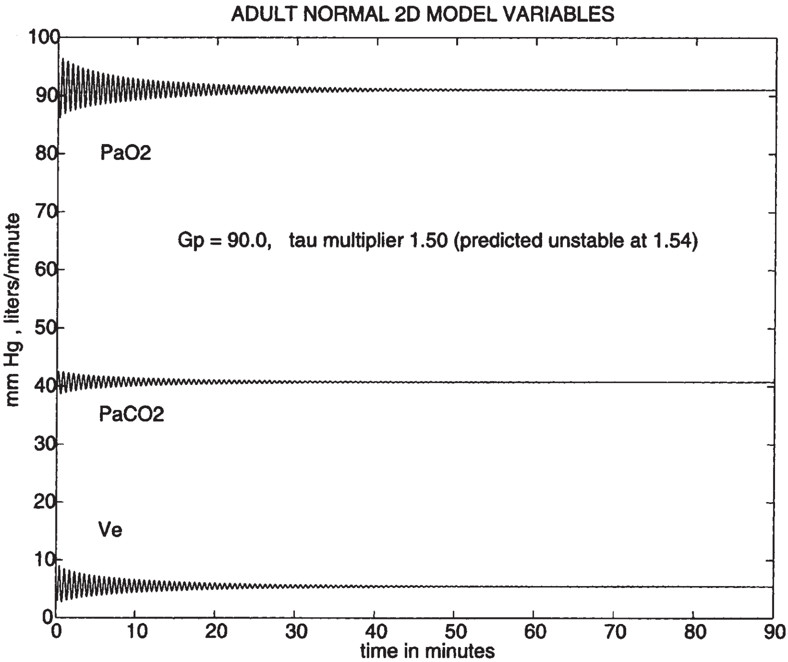

Fig. 5. Stable two-dimensional basic model with high gain.

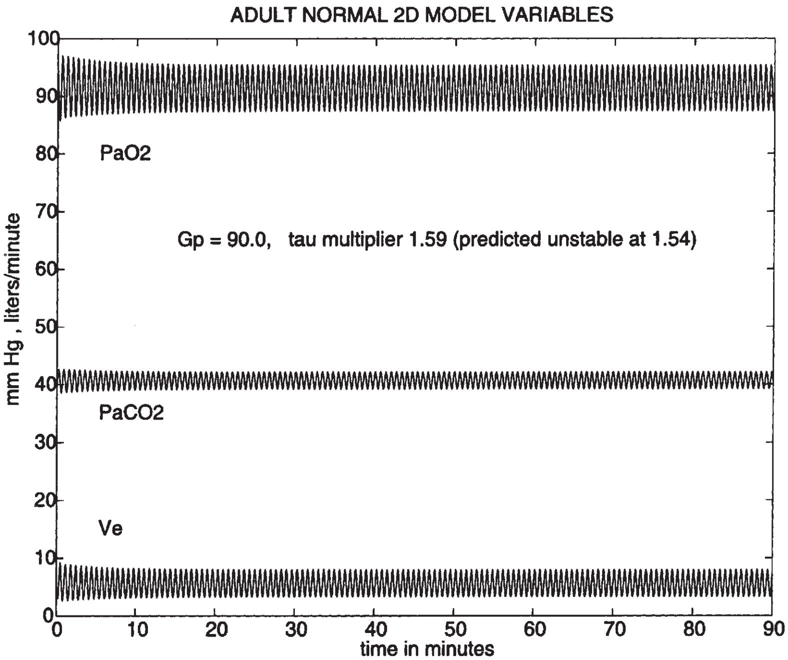

Fig. 6. Unstable two-dimensional basic model with high gain.

the carotid bodies are extremely well supplied with capillaries and thus very efficiently perfused with arterial blood. They are thus able to respond quickly and proportionately to changes in arterial Pa_{CO_2} and Pa_{O_2}.

3.4. A modified control equation for the two-dimensional model

To compensate for this heightened sensitivity to Pa_{CO_2} and Pa_{O_2} we can amend the two-dimensional model presented in Section 3.1 in the following way. Notice that in the five-dimensional model the brain $P_{B_{CO_2}}$ level varies much less than Pa_{CO_2}. Therefore the central control response varies less. We can modify the control equation by including a central control component as follows:

$$V_C = [[\ K_{VC_1} + K_{VC_2}(x(t-\tau) - I_C)\ ]],$$

where K_{VC_1} and K_{VC_2} are constants. Again, the double bracket notation indicates that V_C will be greater than or equal to zero. What we have done is to introduce a second control component which varies much less than the peripheral control for $x(t)$ (i.e. Pa_{CO_2}) levels. In the steady state this would act similarly to the central control. Of course, this setup does not allow V_C to become zero and we assume the same delay but we are concerned here only with a qualitative look at the effects on the steady state calculations. A more correct formulation requires a three-dimensional state space model to allow for a correct formulation of the central control $\dot{V}_{cent}$. We have analyzed this case in Part II of this paper. Table 3 and Figures 7 and 8 give calculated parameter values and simulations results, respectively. In Table 4, we compare the stability conditions as predicted by the model with a peripheral control only versus one with a variable central control component added. We note Table 4 shows that the system with a central control component will be much more stable than one with a peripheral control alone.

3.5. Parameter interaction

The following graphs illustrate the relation between several important determiners of stability versus changing control gain. Figure 9 illustrates how the coefficients k_1 and k_2 from (35) vary versus control gain. We use the modified control equation in Section 3.4 with central drive constant K_{VC_1} set at 3.0 l/min. In this graph k_2 moves from positive to negative values while k_1 remains positive. One reason for this is that $\bar{x}$ and $\bar{y}$ do not vary much with controller gain as can be seen in Figure 10 thus stabilizing k_1. Over a very large set of variations in parameter values it has been the case that k_1 will not be negative unless k_2 is also. Thus it appears that multiple switching in stability does not occur when reasonable physiological parameter values are used.

4. Discussions

It is clear that the central control contributes much to the stable behavior of the human respiratory control system. We can compare the results of the stability analysis

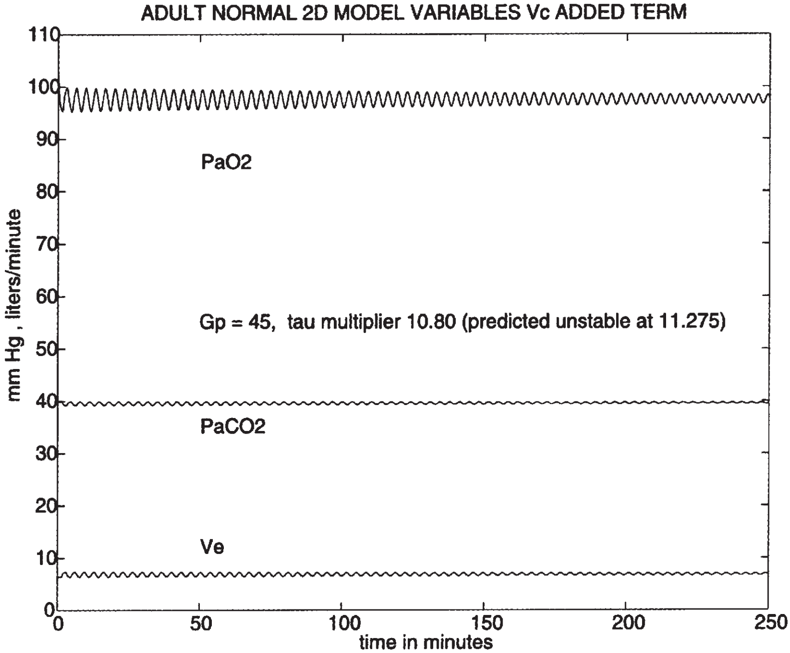

Fig. 7. Stable two-dimensional model with a modified control and moderate gain.

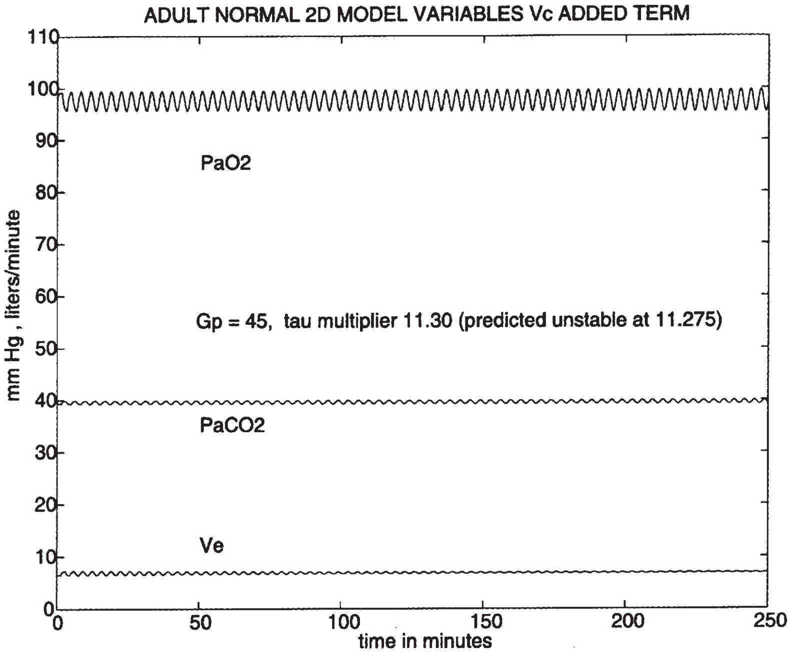

Fig. 8. Unstable two-dimensional model with a modified control and high gain.

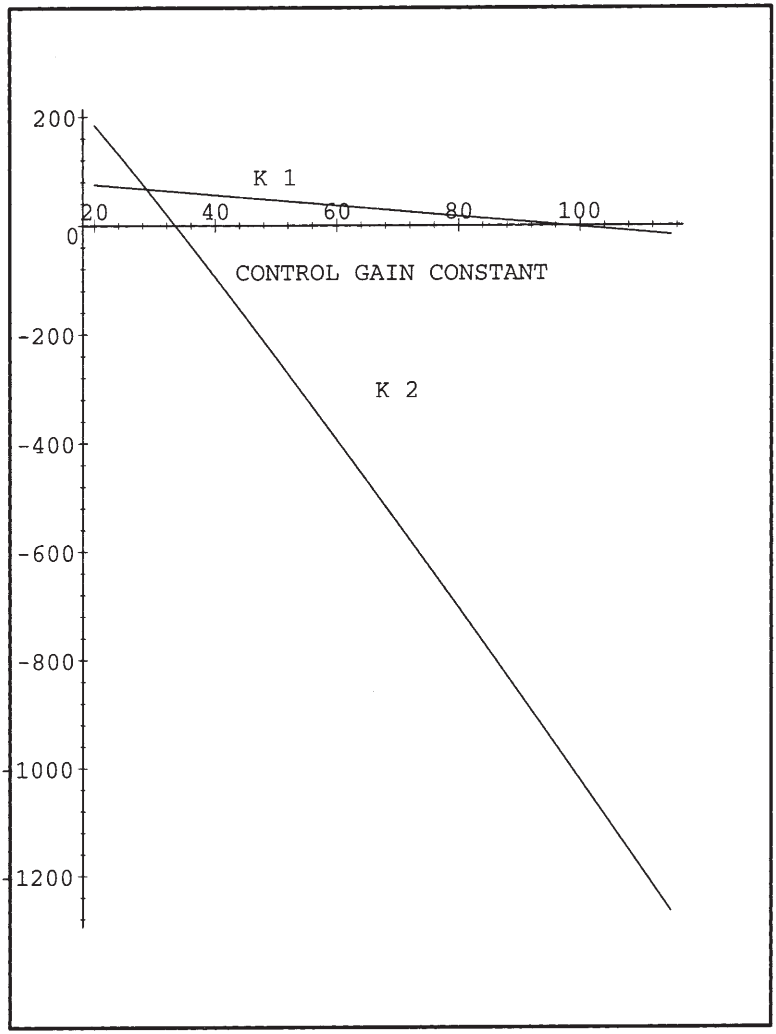

Fig. 9. k_1 and k_2 versus control gain.

for the two-dimensional and five-dimensional models. We compare the two-dimensional model with the modified control equation and varying central gain. Using the parameter values indicated, we see from Table 5 that there is a reasonable correlation in the predictions about stability. Note that for normal control gain the two-dimensional model predicted instability at a τ multiplier of 10.54 while simulations of the five-dimensional gives 14.1. State variables also correlate very well.

We see that the overall structure of instability was illuminated by the smaller models and the actual state variables were in good agreement for the modified central control component. The τ multiplier necessary for instability for the five-dimensional model was about 28% higher than predicted by the smaller models indicating that the tissue compartments add to the stability of the system. Figure 11

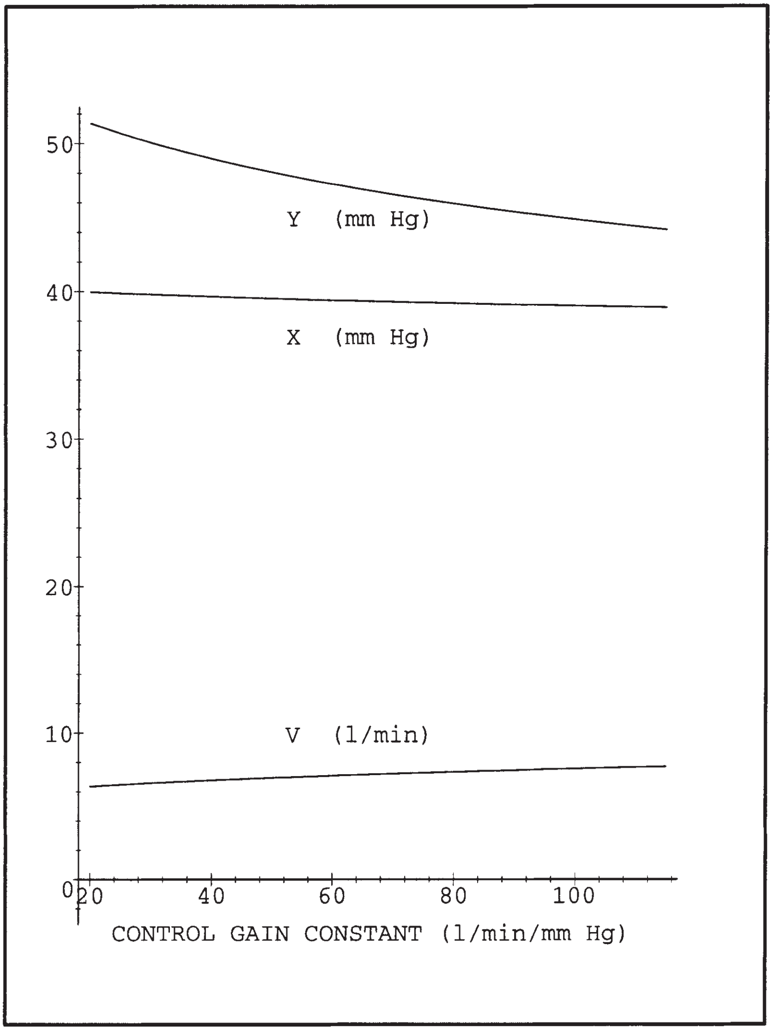

Fig. 10. Two-dimensional steady state values versus control gain.

represents the five-dimensional model simulation at instability. Note that $P_{V_{CO_2}}$ and $P_{V_{O_2}}$ do not vary much even in unstable situations.

Finally, we will present calculations comparing the effects produced by varying different parameters. We will introduce one further parameter in this analysis. We have heretofore used E_F set at 0.7 to reflect dead space ventilation V_D and diffusion inefficiencies. This factor reduces each breath by a certain percentage. In this case, we are assuming that an increase in ventilation rate is produced by increased breathing rate and thus each breath is reduced by the same dead space volume percentage. We might also assume that breathing rate is held constant and depth of breathing is varied. In this case there will be a fixed dead space volume subtracted from each breath. We, therefore, have $V_{eff} = V - V_D$. E_F will be set at 1.0. Notice that in this case V_D serves to reduce V by a fixed amount in each breath.

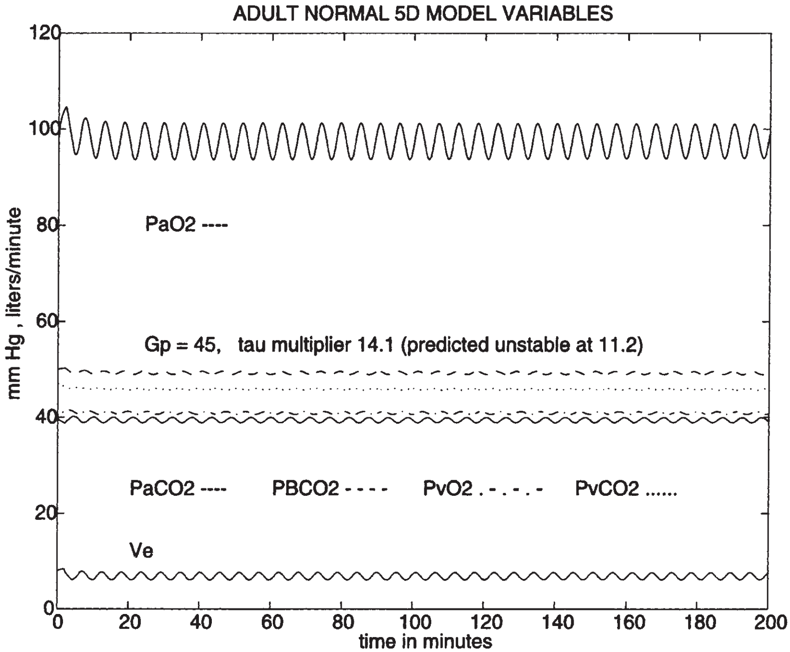

Fig. 11. Unstable simulation of the five-dimensional state space model.

Table 6 presents the results obtained by varying different parameters and their effects on stability. We compile the results for both of the versions of modeling dead space ventilation just described. To develop this table we start with the standard parameter values and the calculated τ^* multiplier for these parameters. Some changes in the steady state values for $P_{V_{CO_2}}$ and $P_{V_{O_2}}$ are to be expected when large changes in parameters are made. We have kept the levels of $P_{V_{CO_2}}$ and $P_{V_{O_2}}$ fixed at the values found in Table 5 for comparison purposes. Column 1 gives the parameter which is changed while others are held fixed. Column 2 gives the change in that parameter by a certain factor. Column 3 gives the factor by which the standard value for the τ^* multiplier is increased or decreased when this parameter change occurs. We see that an increase in lung compartment volumes tends to stabilize the system which agrees with [17]. It is interesting to note that using $V_{eff} = V - V_D$ to represent dead space ventilation acts to reduce the stability of the system more than the factor E_F does. This makes sense if we consider that E_F acts to reduce the effectiveness of the control signal by a certain constant percentage while in the expression $V_{eff} = V - V_D$ the useless volume V_D becomes a smaller percentage as deeper breaths are taken and hence increasing the efficacy of the control. In actuality, the control signal modulates both rate and depth of breathing.

The analytical methods described above can predict the effects of any combination of factors as well. From Table 6, one can ascertain the general effects of any combination of factors.

5. Conclusions

We now conclude this paper with some observations based on the foregoing analysis.

1. We have looked at the behavior of the model when only peripheral control is utilized. In this case, the delay needed to produce instability is much smaller than is expected from observations and experiments. Introducing a second term to mimic the central control near steady state dramatically increases the stability of the system. This form of central control is not physiologically correct but indicates the role played by the actual central control in stabilizing the respiratory control system.
2. Further analysis with modified controls which mimic both central and peripheral control can be combined with the above two-dimensional model to study stability properties. Such a control might be as is given in [3] where a convolution was used to smooth out the instability of a peripheral control which responds instantaneously to variations in arterial blood gas levels. A control which incorporates the effects of both $P_{a_{CO_2}}$ and $P_{a_{O_2}}$ (such as suggested in [5]) can also be analyzed using the above described results.
3. The central control acts to reduce the instability inherent in the peripheral control mechanism. One might be tempted to believe that the central control evolved for this purpose. The peripheral control responds quickly to changes in the blood gases while the central control responds more slowly and with less variation due to the process of transforming $P_{a_{CO_2}}$ levels into $P_{B_{CO_2}}$ levels. Peripheral response is most critical during hypoxia and in such cases quick changes in ventilation are necessary. Quick changes to increased $P_{a_{CO_2}}$ and hence decreases in pH levels are also important. The price paid for this response is instability and the central control acts to mitigate this factor.
4. The tissue compartments act to dampen oscillations and contribute to stability as Table 5 indicates. Notice that the five-dimensional model seems to be more stable than the two-dimensional model. Also, Table 6 indicated an increase in lung compartment volumes acts to stabilize the system. However, with the controls presented the effects of changes in lung volumes are much larger than predicted in [16].
5. Variations in controller gain are critical to the stability of the system.
6. A control which varies depth of breathing is more unstable than one which varies rate of breathing.

References

1. Batzel, J.J., Tran, H.T.: Modeling variable delay and instability in the control system for human respiration: Applications to infant non-rem sleep. J. of Applied Math. and Computation, **110**, 1–51 (2000)
2. Boese, F.G.: Comments on “On the zeros of some transcendental equations” by K.L. Cooke and P. van den Driessche, preprint
3. Carley, D.W., Shannon, D.C.: A minimal mathematical model of human periodic breathing. J. Appl. Physiol., **65** (3), 1400–1409 (1988)

4. Cleave, J.P., Levine, M.R., Fleming, P.J., Long, A.M.: Hopf bifurcations and the stability of the respiratory control system. J. Theor. Biol., **119**, 299–318 (1986)
5. Cooke, K., Turi, J.: Stability, instability in delay equations modeling human respiration. J. Math. Biol., **32**, 535–543 (1994)
6. Cooke, K., van den Driessche, P.: On zeroes of some transcendental equations. Funkcialaj Ekvacioj **29**, 77–90 (1986)
7. Cunningham, D.C., Robbins, P.A., Wolff, C.B.: Integration of respiratory responses. Handbook of Physiology. The Respiratory System, Part II Fishman A.P. ed. American Physiol. Soc., Bethesda Md., 475–528 (1986)
8. Dieudonne, J.: Foundations of Modern Analysis. Academic Press, N.Y. (1960)
9. Elhefnawy, A., Saidel, G.M., Bruce, E.N.: CO_2 control of the respiratory system: plant dynamics and stability analysis. Annals of Biomed. Eng., **16**, 445–461 (1988)
10. El'sgol'ts, L.E., Norkin, S.B.: Introduction to the Theory and Applications of Differential Equations with Deviating Arguments. Academic Press, N.Y. (1973)
11. Glass, L., Mackey, M.C.: Pathological conditions resulting from instabilities in physiological control systems. Annal. N.Y. Acad. Sci., **316**, 214–235 (1979)
12. Grodins, F.S., Buell, J., Bart, A.J.: Mathematical analysis and digital simulation of the respiratory control system. J. Appl. Physiology, **22** 2, 260–276 (1967)
13. Guyton, A.C.: Physiology of the Human Body. Saunders, Philadelphia (1984)
14. Hale, J.K., Verduyn Lunel, S.M.: Introduction to Functional Differential Equations. Springer-Verlag, N.Y. (1993)
15. Khoo, M.C.K: Periodic breathing. The Lung: scientific foundations. Grystal R. G. and West J.B. et al. Raven Press Ltd., New York, 1419–1431 (1991)
16. Khoo, M.C.K., Gottschalk, A., Pack, A.I.: Sleep-induced periodic breathing and apnea: A theoretical Study. J. Applied Physiol., **70** 5, 2014–2024 (1991)
17. Khoo, M.C.K, Kronauer, R.E., Strohl, K.P., Slutsky, A.S.: Factors inducing periodic breathing in humans: a general model. J. Appl. Physiol., **53** 3, 644–659 (1982)
18. Kuang, Y.: Delay Differential Equations with Applications in Population Dynamics (1993) Mathematics in Science and Engineering 191-Academic Press, Boston Mass.
19. Mackey, M.C., Glass, L.: Oscillations and chaos in physiological control systems. Science **197**, 287–289 (1977)
20. West, J.B.: Respiratory Physiology. Williams and Willaims Co. (1979)

Appendix

Table 1. Stability calculation parameters for Figures 3 and 4.

Quantity	Unit	Value
G_P	l/min/mmHg	45.0
$\dot{Q}$	l/min	6.0
ω_o	......	7.47
Normal τ	sec	8.5
Unstable τ multiplier	......	2.02
$\bar{x}$	mmHg	41.48
$\bar{y}$	mmHg	66.9
$\bar{V}$	l/min	4.59
$\bar{x}\bar{V}_X + \bar{y}\bar{V}_Y$	.....	44.7
$A_1^2B_1^2 - (A_2B_1 + A_1B_2)^2$	......	−2738.8

$P_{V_{CO_2}} = 46.0$ $P_{V_{O_2}} = 40.9$ $P_{I_{O_2}} = 150.0$

Table 2. Stability calculation parameters for Figures 5 and 6.

Quantity	Unit	Value
G_P	l/min/mmHg	90.0
$\dot{Q}$	l/min	6.0
ω_o	......	9.7
Normal τ	sec	8.5
Unstable τ multiplier	....	1.54
$\bar{x}$	mmHg	40.7
$\bar{y}$	mmHg	59.0
$\bar{V}$	l/min	5.45
$\bar{x}\bar{V}_X + \bar{y}\bar{V}_Y$	.....	54.8
$A_1^2B_1^2 - (A_2B_1 + A_1B_2)^2$	......	−3667.3

$P_{V_{CO_2}} = 46.0$ $P_{V_{O_2}} = 40.9$ $P_{I_{O_2}} = 150.0$

Table 3. Stability calculation parameters for Figures 7 and 8.

Quantity	Unit	Value
Figure 7		
G_P	l/min/mmHg	45.0
K_{VC_1}	l/min	3.0
K_{VC_2}	....	0.5
$\dot{Q}$	l/min	6.0
ω_o	......	1.765
Normal τ	sec	8.5
Unstable τ multiplier	...	11.27
$\bar{x}$	mmHg	39.57
$\bar{y}$	mmHg	48.46
$\bar{V}$	l/min	6.85
$P_{V_{CO_2}}$	l/min	46.0
$P_{V_{O_2}}$	l/min	41.0
$P_{I_{CO_2}}$	l/min	146.0
$\bar{x}\bar{V}_X + \bar{y}\bar{V}_Y$	.....	37.14
$A_1^2 B_1^2 - (A_2 B_1 + A_1 B_2)^2$	......	−168.62
$A_1^2 + B_1^2 - (A_2 + B_2)^2$	......	51.03
Figure 8		
G_P	l/min/mmHg	90.0
K_{VC_1}	l/min	3.0
K_{VC_2}	....	0.5
$\dot{Q}$	l/min	6.0
ω_o	......	5.08
Normal τ	sec	8.5
Unstable τ multiplier	....	3.524
$\bar{x}$	mmHg	39.09
$\bar{y}$	mmHg	45.36
$\bar{V}$	l/min	7.5
$P_{V_{CO_2}}$	l/min	46.0
$P_{V_{O_2}}$	l/min	41.0
$P_{I_{CO_2}}$	l/min	146.0
$\bar{x}\bar{V}_X + \bar{y}\bar{V}_Y$	.....	47.93
$A_1^2 B_1^2 - (A_2 B_1 + A_1 B_2)^2$	......	−862.24
$A_1^2 + B_1^2 - (A_2 + B_2)^2$	......	7.49

Table 4. Stability comparison for 2-D model: different control equations.

Quantity	Peripheral control only	Varying V_C
Moderate G_P comparisons		
G_P	45	45.0
K_{VC_1}	....	3.0
K_{VC_2}	....	0.5
ω_o	7.69	1.76
Normal τ	8.5	8.5
Unstable τ multiplier	1.97	11.27
$\bar{x}$	41.35	39.57
$\bar{y}$	64.0	48.46
$\bar{V}$	4.74	6.85
$P_{V_{O_2}}$	41.0	41.0
$P_{V_{CO_2}}$	46.0	46.0
$P_{I_{O_2}}$	146.0	146.0
High G_P comparisons		
Quantity	Peripheral control only	Varying V_C
G_P	90	90.0
K_{VC_1}	....	3.0
K_{VC_2}	....	0.5
ω_o	10.2	5.1
Normal τ	8.5	8.5
Unstable τ multiplier	1.47	3.53
$\bar{x}$	40.6	39.09
$\bar{y}$	56.2	45.35
$\bar{V}$	5.6	7.45
$P_{V_{O_2}}$	41.0	41.0
$P_{V_{CO_2}}$	46.0	46.0
$P_{I_{O_2}}$	146.0	146.0

Table 5. Stability calculation comparisons for 2-D and 5-D models.

Quantity	2-D	5-D
G_C	...	1.2
G_P	45.0	45.0
V_C added term	$3 + 0.5\bar{x}$	....
$\dot{Q}$	6.0	6.0
ω_o	1.88	...
Normal τ	8.5	8.5
Unstable τ multiplier	10.54	14.1*
$\bar{x}$	39.45	39.46
$\bar{y}$	48.98	48.53
$\bar{V}$	6.78	6.12
$P_{V_{CO_2}}$	45.8	45.8
$P_{V_{O_2}}$	40.9	40.9
$P_{I_{O_2}}$	146.0	146.0

* numerical estimate

Table 6. Stability results of parameter changes: 2-D model with modified control.

2-D with $E_F = 0.7$ Quantity	Parameter multiplier	τ^* multiplier
G_P	1.0	11.27 x
G_P	2.0	3.53 x
$M_{L_{CO_2}}$ and $M_{L_{O_2}}$	0.5	5.60 x
$M_{L_{CO_2}}$ and $M_{L_{O_2}}$	2.0	22.6 x
2-D with $V_D = 2.0$ l/min Quantity	**Parameter multiplier**	**τ^* multiplier**
G_P	1.0	2.63 x
G_P	2.0	1.43 x
$M_{L_{CO_2}}$ and $M_{L_{O_2}}$	0.5	1.3 x
$M_{L_{CO_2}}$ and $M_{L_{O_2}}$	2.0	5.27 x

$P_{V_{CO_2}} = 46.0$ $P_{V_{O_2}} = 41.0$ $P_{I_{O_2}} = 146.0$

Table 7. Parameter values for 2-D model.

Quantity	Unit	Value
G_P	l/min/mmHg	45.0
$\dot{Q}$	l/min	6.0
$\dot{Q}_B$	l/min	0.75
$P_{V_{CO_2}}$	mmHg	46.0
$P_{V_{O_2}}$	mmHg	41.0
$P_{I_{O_2}}$	mmHg	146.0[a]
$I_P,\ I_C$	mmHg	35.0
$M_{L_{CO_2}}$	liter	3.2
$M_{L_{O_2}}$	l/min	2.5
EF	.....	0.7
K_{CO_2}	$l_{STPD}/(l\ mmHg)$	0.0057
m_a	$l_{STPD}/(l\ mmHg)$	0.00025
B_a	l_{STPD}/l	0.1728
m_v	$l_{STPD}/(l\ mmHg)$	0.0021
B_v	l_{STPD}/l	0.0662

[a] includes 4 mmHg alveolar arterial gradient